

Boost-invariant Hamiltonian approach to heavy quarkonia

Stanisław D. Głązak and Jarosław Młynik

Institute of Theoretical Physics, Warsaw University, ul. Hoża 69, 00-681 Warsaw, Poland

(Dated: 23 June 2006)

Light-front Hamiltonian formulation of QCD with only one flavor of quarks is used in its simplest approximate version to calculate masses and boost-invariant wave functions of $c\bar{c}$ or $b\bar{b}$ mesons. The quark-antiquark Hamiltonian is obtained in the lowest (second) order of a weak-coupling expansion scheme for Hamiltonians of effective particles in quantum field theory. It is shown that in the simplest version the strong coupling constant α and quark mass m (for suitable values of the renormalization group parameter λ that is used in the calculation), can be adjusted so that a) masses of 12 lightest well-established $b\bar{b}$ mesons are reproduced with accuracy better than 0.5% for all of them, which means 50 MeV in a few worst cases and on the order of 10 MeV in other cases, or b) masses of 11 lightest $c\bar{c}$ mesons are reproduced with accuracy better than 3% for all of them, which means better than 100 MeV in a few worst cases and on the order of 10 MeV in the other cases, while the parameters α and m are near the values expected in the cases a) and b) by analogy with other approaches. A 4th-order study in the same Hamiltonian scheme will be required to explicitly include renormalization group running of the parameters α and m from the scale set by masses of bosons W and Z down to the values of λ that are suitable in the bound-state calculations. In principle, one can use the Hamiltonian approach to describe the structure, decay, production, and scattering of heavy quarkonia in all kinds of motion, including velocities arbitrarily close to the speed of light. This work is devoted exclusively to a pilot study of masses of the quarkonia in the simplest version of the approach.

PACS numbers: 12.38.Aw, 11.15.Tk, 12.38.Lg

I. INTRODUCTION

In the Hamiltonian approach to QCD that is employed here, the calculation of masses of heavy quarkonia does not involve the well-known notions of scattering states for quarks and gluons, Feynman diagrams, path integral, euclidicity postulate, lattice gauge theory, or non-trivial vacuum expectation values. Instead, a renormalization group procedure for effective particles in quantum field theory (RGPEP, see below) is applied to quarks and gluons in canonical light-front (LF) QCD and leads to an effective Hamiltonian whose eigenvalue problem is expected to provide a first approximation to the true dynamics of the theory. The eigenvalues of the Hamiltonian are equal to the masses of the quarkonia (actually, squares of the masses) instead of their energies in a specific frame of reference. The approximate dynamical picture studied here can be valid only for a set of states at the low end of the mass spectrum.

The LF formalism is developed in a Fock space. Creation and annihilation operators for effective quarks and gluons are calculable in a perturbative expansion using RGPEP (a brief review of the method is provided in the next section) and the basis states in the Fock space are formed by acting with the calculable creation operators on the state of vacuum. The effective Hamiltonian eigenvalue problem exists in the momentum representation and would not be local if one attempted to write it in a position space. Nevertheless, the simplest approximate momentum-space dynamics respects not only the boost symmetry but also the rotational symmetry. Therefore, one can describe the structure of lowest-mass eigenstates corresponding to well-known $b\bar{b}$ and $c\bar{c}$ mesons using the

spectroscopic scheme that is quite analogous to the one adopted in non-relativistic quantum mechanics with potential forces that respect rotational symmetry in a meson center-of-mass frame of reference. Thus, the LF approach has a potential to be helpful in solving conceptual problems with Poincaré symmetry in quantum theories [1, 2] and the results described here can be considered an indicator of existence of a reasonable candidate for a new expansion method for solving theories as complex as QCD [3]. However, the approach is still in its infancy. The crude, heuristic study described here is merely a small step that needs to be taken on the way to find out if the RGPEP can work for heavy quarkonia in LFQCD as outlined in [4].

Since the beginning of the theory of $c\bar{c}$ system [5, 6, 7, 8], through the development of potential models [9, 10, 11, 12, 13, 14, 15, 16, 17, 18] and studies based on effective Lagrangians [19, 20, 21], the latter method known also to work well in Hamiltonian approach to QED [22, 23], current understanding of heavy quarkonia, especially in lattice approach [24, 25, 26], is one of the best examples of great progress achieved in theory of strong interactions [27]. In the wake of the development, conceptual problems with a relativistic description of hadrons in the Minkowski space and questions concerning the structure of the vacuum state continue to bother theorists [3, 28]. The problem is how to derive a quantum Hamiltonian for quarks and gluons that precisely describes hadronic states in agreement with special relativity.

One can write a formal expression for a Hamiltonian of quarks and gluons using various forms of dynamics [1]. In the standard form, one describes the evolution of a

system of particles using the time parameter t , which is measured along a time-like direction in space-time. But the formal expression must be regulated and renormalized, and one has to explain how to define the ground state of the theory that supports the tower of excitations that represent all kinds of relativistically moving and interacting hadrons. None of these tasks has been completed yet with the desired clarity and precision. In the LF form of dynamics, one uses a “time” parameter that is conventionally denoted by $x^+ = t + z$. Since the LF hyperplane $x^+ = 0$ is preserved by boosts along z -axis, and also by two other boost-like transformations, the LF form of Hamiltonian dynamics is invariant under the three special boosts. The three boosts are prerequisite to the construction of hadronic states in all kinds of motion. The boost symmetry rises hope that the LF Hamiltonian dynamics can help in finding a universal theoretical description of hadrons in all frames of reference, including both their center-of-mass frame (CMF), in which the constituent quark model is developed [29], and the infinite momentum frame (IMF), in which the concept of partons is developed [30]. The exact description of a hadron in motion is also essential in exclusive (or semi-exclusive) processes [31]. Regarding the vacuum, the ground state problem in QCD does not appear in the LF form of dynamics in the way known from the standard approach [28, 32] and the LF Hamiltonian dynamics of quarks and gluons is of great interest to many researchers [33], as a serious alternative to the standard form. However, LFQCD challenges theoreticians with basic questions concerning quantum mechanics of particles and fields and relativity.

In search for understanding of the quark-gluon dynamics, it is natural to consider quantum chromodynamics of only heavy quarks coupled to gluons. A quark is considered heavy when the phenomenological mass parameter associated with the quark, m , is much larger than Λ_{QCD} , the latter being defined in the RGPEP procedure that one can use to evaluate effective LF Hamiltonians [34]. The restriction to only heavy quarks creates a situation in which the renormalization group parameter, denoted by λ , can be simultaneously much smaller than m and much larger than Λ_{QCD} . In such circumstance, the effective color coupling constant at scale λ , g_λ , can be formally considered small in comparison to 1 even when λ is much smaller than m . The smallness of the coupling constant implies that the LF Hamiltonian of QCD expressed in terms of the effective quark degrees of freedom corresponding to $\lambda \ll m$, denoted by H_λ , can be evaluated in RGPEP using perturbation theory. But the price to pay for this simplification is high because the quenched heavy-flavor version of the theory must be incomplete; it misses dynamical interplay among different flavors and entirely ignores effects due to light quarks. On the other hand, the price is worth paying because the single heavy flavor theory quickly renders a simple dynamical picture that may be helpful in learning more about LF QCD. Namely, it is sufficient to consider H_λ obtained in just

2nd-order perturbation theory and augment it with an ansatz for the mass gap for effective transverse gluons and these two steps already render a boost-invariant eigenvalue equation in the effective quark-antiquark Fock sector which has a well-defined and phenomenologically attractive structure [4]: the Coulomb potential with Breit-Fermi corrections is supplemented with a harmonic oscillator term with a frequency ω that is explicitly related to the values of α and m at the scales λ at which this structure may be valid, which turns out to be the scale corresponding to the distances between quarks not much larger than the size of the lowest-mass mesons. At larger distances, additional gluons may be created and the potential may become linear, as will be discussed later.

The resulting dynamical picture for the low-mass states is not sensitive to the details of the mass gap ansatz for effective gluons that was used to finesse the picture. Therefore, in order to begin a study of the true mass gap for gluons that may undergird the finessed effective picture, one needs to complete the 4th-order calculation of H_λ using RGPEP. A major problem in the 4th-order calculation is to include light quarks. It would be helpful to know if the light quarks should be expected to introduce significant effects in the LF dynamics of heavy quarks. But even before the inclusion of light quarks, a glimpse of the magnitude of the necessary 4th-order effects could be obtained already in one-flavor QCD by comparison of the 2nd-order picture with the 4th-order one. In particular, the 4th-order terms matter in obtaining rotational symmetry. Unfortunately, a 4th-order calculation requires understanding of many terms in the LF Hamiltonian of QCD at once.

However, in the limit of m large in comparison to λ that itself is still much larger than Λ_{QCD} , one can considerably simplify the calculation of quark Hamiltonians using RGPEP. One can compute a 2nd-order Hamiltonian that acts only in the effective heavy quark-antiquark sector, $H_{Q\bar{Q}\lambda}$, and evaluate interactions in $H_{Q\bar{Q}\lambda}$ that depend on the quark spin. The result is that the leading spin-dependent terms that one obtains from the 2nd-order RGPEP, in addition to the Coulomb potential and the harmonic oscillator force, automatically respect rotational symmetry. Thus, there is a chance to learn if the effective 2nd-order dynamics can fit some data even before one calculates the required 4th-order terms. One may ask how hard it is to obtain the observed spectrum of masses of $c\bar{c}$ and $b\bar{b}$ mesons using the 2nd-order Hamiltonian picture. The simplest-version study described here provides a surprisingly optimistic answer. Not only the masses that one hopes to be reproducible relatively well turn out to be reproducible very well, but also those masses that one expects to be reproducible rather poorly turn out to be reproducible with considerably less accuracy than those that are reproduced well. The results seem to match data in a pattern that agrees with expectations concerning accuracy of the simplest version of the approach.

Section II briefly describes the derivation of the effec-

tive Hamiltonians studied here. The leading approximation to the heavy quark eigenvalue problem is explained in Section III. Section IV discusses spin effects and lists eigenvalue equations that describe mesons with spin 0, 1, and 2, with orbital angular momenta equal 0, 1, 2, or 3. Masses and wave functions of mesons that are obtained by numerical solution of these equations are discussed in Section V. Conclusions are summarized in Section VI. Key details of the calculations are relegated to Appendices.

II. BOOST-INVARIANT HAMILTONIANS

This section explains how the boost-invariant Hamiltonians for heavy quarkonia that are used in the next sections to evaluate masses of $c\bar{c}$ and $b\bar{b}$ mesons are derived in QCD [4].

A. Canonical LF QCD

One begins from the standard Lagrangian of color gauge theory with one flavor of quarks of mass m ,

$$\mathcal{L} = \bar{\psi}(i\mathcal{D} - m)\psi - \frac{1}{4}F^{\mu\nu a}F_{\mu\nu}^a. \quad (1)$$

The corresponding generator of evolution in x^+ in the gauge $A^+ = 0$ takes the form

$$\begin{aligned} \mathcal{H}_{can} = & H_{\psi^2} + H_{A^2} + H_{A^3} + H_{A^4} + H_{\psi A \psi} \\ & + H_{\psi A A \psi} + H_{[\partial A A]^2} + H_{[\partial A A](\psi \psi)} + H_{(\psi \psi)^2}, \end{aligned} \quad (2)$$

where each of the terms is an integral of a corresponding Hamiltonian density \mathcal{H} over the LF hyperplane, $H_i = \int dx^- d^2x^\perp \mathcal{H}_i$. Four terms that explicitly enter in the derivation of the approximate 2nd-order boost-invariant effective theory for heavy quarkonia, are

$$\mathcal{H}_{\psi^2} = \frac{1}{2}\bar{\psi}\gamma^+ \frac{-\partial^\perp 2 + m^2}{i\partial^+}\psi, \quad (3)$$

$$\mathcal{H}_{A^2} = -\frac{1}{2}A^\perp(\partial^\perp)^2 A^\perp, \quad (4)$$

$$\mathcal{H}_{\psi A \psi} = g\bar{\psi}\mathcal{A}\psi, \quad (5)$$

$$\mathcal{H}_{(\psi \psi)^2} = \frac{1}{2}g^2\bar{\psi}\gamma^+ t^a \psi \frac{1}{(i\partial^+)^2} \bar{\psi}\gamma^+ t^a \psi. \quad (6)$$

Other terms in the canonical Hamiltonian are also important. For example, the three-gluon coupling term plays an implicit role as a seed of the renormalization group flow of the coupling constant. This effect becomes explicit first in 3rd-order calculations [35].

At $x^+ = 0$, the fermion field

$$\psi = \sum_{\sigma c} \int [k] \left[\chi_c u_{k\sigma} b_{k\sigma c} e^{-ikx} + \chi_c v_{k\sigma} d_{k\sigma c}^\dagger e^{ikx} \right], \quad (7)$$

and the gluon field

$$A^\mu = \sum_{\sigma c} \int [k] \left[t^c \varepsilon_{k\sigma}^\mu a_{k\sigma c} e^{-ikx} + t^c \varepsilon_{k\sigma}^{\mu*} a_{k\sigma c}^\dagger e^{ikx} \right], \quad (8)$$

are quantized by imposing commutation relations

$$\begin{aligned} \{b_{k\sigma c}, b_{k'\sigma'c'}^\dagger\} &= \{d_{k\sigma c}, d_{k'\sigma'c'}^\dagger\} \\ &= 16\pi^3 k^+ \delta_{\sigma\sigma'} \delta_{cc'} \delta^3(k - k'), \end{aligned} \quad (9)$$

$$\left[a_{k\sigma c}, a_{k'\sigma'c'}^\dagger \right] = 16\pi^3 k^+ \delta_{\sigma\sigma'} \delta_{cc'} \delta^3(k - k'). \quad (10)$$

The measure of integration over momenta, $[k]$, is $\theta(k^+) dk^+ d^2 k^\perp / (16\pi^3 k^+)$ and the LF three-momentum δ -function is $\delta^3(k - k') = \delta(k^+ - k'^+) \delta(k^\perp - k'^\perp) \delta(k^2 - k'^2)$. Spins are denoted by σ and colors by c . Further details concerning our notation can be found in the Appendix (see also Ref. [4]).

B. Regularization

The canonical Hamiltonian is divergent and the RG-PEP begins with regularization of the ultra-violet and small- k^+ divergences. The ultraviolet divergences result from integrating over large transverse momenta of quanta in the intermediate states when one attempts to evaluate powers of the Hamiltonian. In 3+1 dimensional theory, the quadratically and logarithmically diverging transverse integrals result from momentum dependent spin factors for fermions and vector bosons. The small- k^+ divergences arise due to gauge couplings of gluons. Note that in the $A^+ = 0$ gauge only A^\perp and $\psi^+ = \frac{1}{2}\gamma^0\gamma^+\psi$ are dynamical variables. In particular, A^- depends on A^\perp and ψ^+ . As a consequence, interaction terms in the Hamiltonian can be written using the polarization vector ε^μ for gluons whose only two transverse components are independent degrees of freedom. A gluon with momentum k^+ and k^\perp has $\varepsilon^- = 2\varepsilon^\perp k^\perp/k^+$. The k^+ in denominator in ε^- is a source of small- k^+ singularities in LF QCD. There exist similar small- k^+ singularities in the instantaneous interactions along z -axis on the LF hyperplane, especially where $1/\partial^+ 2$ appears, which happens similarly to how the inverse of a three-dimensional Laplacian appears in the familiar Coulomb potential in the standard approach. The small- k^+ singularities also occur in a 1+1 dimensional theory [36].

In the boost-invariant formulation of LF QCD, one regulates the theory not by limiting the momentum components k^\perp and k^+ of every individual quark and gluon separately. Instead, only the relative momenta of particles in the interaction terms are limited. The regularization is accomplished by insertion of regulating factors r in vertices, see [4]. The overarching rule for construction of the regulating factors r is that they must respect 7 kinematical symmetries of the LF scheme. This rule is analogous to the requirement of rotational symmetry in the standard approach. There is a factor $r = r_\Delta r_\delta$,

for every bare particle in every vertex. r_Δ limits the range of the relative transverse momentum of an interacting bare particle with respect to other particles participating in the interaction. The limit is set by the parameter Δ . If a particle of momentum k carries a fraction x of the total p^+ of particles in an interaction term, $k^+ = xp^+$, then its relative transverse momentum with respect to the particles interacting in this term is defined as $\kappa^\perp = k^\perp - xp^\perp$, where p^\perp is the sum of transverse momenta of all particles annihilated or created in the term. We use $r_\Delta = \exp(-\kappa^\perp 2/\Delta^2)$, and the ultraviolet regularization parameter Δ is sent to infinity in comparison to all physical momentum scales, cf. [37, 38].

In the case of the small- k^+ singularities, the regulating factors r_δ limit the ratio $x = k^+/p^+$ by the positive arbitrarily small dimensionless parameter δ . All that is required of the factors r_δ is that they vanish as x^δ when $x \rightarrow 0$. This condition is sufficient in globally colorless states. Linear divergences at small x cancel out and one only needs to take care of the logarithmic divergences in integrals of the type $\int dx/x$. The small- x divergences in the gauge boson dynamics occur in both ultraviolet and infrared regimes. Massless particles can simultaneously have small x and small κ^\perp and their virtuality in the small- x region can be large or small depending on the ratio of $|\kappa^\perp|$ to \sqrt{x} . Small x implies large virtuality only for particles with non-zero mass or fixed κ^\perp .

Once the canonical Hamiltonian is regulated, one needs to introduce counterterms to restore the physics that existed outside the cutoff range and remove effects of the regularization. For example, one inserts mass and vertex counterterms and they remove dependence on the artificial ultraviolet regularization factors r_Δ . The resulting regulated Hamiltonian with counterterms,

$$H = [H_{can} + H_{CT}]_{reg}, \quad (11)$$

provides the starting point for further steps. The further steps are also helpful in establishing the structure of the required counterterms. Note that the dynamics of color-singlet states of finite size should not be sensitive to the small- x regularization. Namely, the singular limit $x \rightarrow 0$ concerns gluons with long wavelengths in the direction of x^- . But the strength of the coupling of such gluons to a finite-size color-neutral pair of quarks should disappear when the wavelength becomes infinitely larger than the distance between the quarks.

C. Effective particles

The initial Hamiltonian H of Eq. (11) is expressed in terms of the creation and annihilation operators defined by the Fourier components of local fields in Eqs. (7) and (8). The same H can be expressed in terms of creation and annihilation operators for effective quarks and gluons that correspond to a renormalization group scale λ in RGPEP. The procedure is constructed in such a way that

when λ tends to infinity, one returns to the canonical operators, but when λ is near the energy-scale of the binding mechanism, on the order of masses of hadrons, the operators should create or annihilate effective particles that correspond to the constituent quarks and gluons. The quantum numbers of the constituents are the same as in the local theory and one assumes that the corresponding creation and annihilation operators are related by a unitary transformation

$$q_\lambda = U_\lambda q_{can} U_\lambda^\dagger, \quad (12)$$

where the same letter q is used for both creation and annihilation operators. The next step is to express H in terms of q_λ instead of q_{can} ,

$$H_\lambda(q_\lambda) = [H_{can} + H_{CT}]_{reg}(q_{can}). \quad (13)$$

The Hamiltonian H remains the same but the coefficients in the expansion in powers of q_λ are new. They include potentials whose structure can be calculated order-by-order in perturbation theory using the RGPEP. The key feature is that H_λ has the structure [39]

$$H_\lambda = f_\lambda G_\lambda, \quad (14)$$

where f_λ denotes form factors of width λ and G_λ represents interaction vertices that can be calculated for any assumed shape of f_λ . The shape we use here is best described using the example of a term in which an effective quark emits an effective gluon:

$$G_\lambda = \int [123] G_\lambda(1, 2, 3) a_{\lambda 1}^\dagger b_{\lambda 2}^\dagger b_{\lambda 3}, \quad (15)$$

$$f_\lambda G_\lambda = \int [123] f_\lambda(123) G_\lambda(1, 2, 3) a_{\lambda 1}^\dagger b_{\lambda 2}^\dagger a_{\lambda 3}, \quad (16)$$

$$f_\lambda(123) = \exp[-(\mathcal{M}_{12}^2 - \mathcal{M}_3^2)^2/\lambda^4]. \quad (17)$$

The invariant masses are defined by the formulas $\mathcal{M}_{12}^2 = (k_1 + k_2)^2$, $\mathcal{M}_3^2 = k_3^2$, using masses in the Lagrangian with $g = 0$ to evaluate minus components of the four-momenta; the quark mass is m and the gluon mass is 0.

The operator G_λ is defined by the coefficients of its expansion in a series of powers of operators q_λ . One can also define \mathcal{G}_λ , which is a series with the same coefficients but q_λ replaced by q_{can} . Then, one can use the constant operator basis q_{can} when solving differential equations of RGPEP for the coefficients, see [34]. \mathcal{G}_λ is split into two parts: \mathcal{G}_0 and $\mathcal{G}_I = \mathcal{G} - \mathcal{G}_0$. \mathcal{G}_0 is the part that does not depend on the coupling constant g . The RGPEP differential equation for \mathcal{G}_I (prime denotes differentiation with respect to λ) is:

$$\mathcal{G}'_I = [f\mathcal{G}_I, \{(1-f)\mathcal{G}_I\}'_{\mathcal{G}_0}], \quad (18)$$

where the curly bracket with subscript \mathcal{G}_0 is introduced to indicate the operator \mathcal{T} that solves equation $[\mathcal{T}, \mathcal{G}_0] =$

$[(1-f)\mathcal{G}_I]'$. The initial condition is that $\mathcal{G}_\infty = H$, and the solution is

$$\mathcal{G}_\lambda = H + \int_\infty^\lambda ds [f_s \mathcal{G}_{Is}, \{[(1-f_s)\mathcal{G}_{Is}]'\}_{\mathcal{G}_0}] . \quad (19)$$

The solution is evaluated order-by-order in powers of the coupling constant g_λ that appears in the vertices of G_λ [35]. The perturbative expansion is legitimate because one never encounters small energy denominators. This feature is secured by the structure of the RGPEP equations and the shape of the form factor f (see the original literature). G_λ is obtained from \mathcal{G}_λ by replacing q_{can} by q_λ .

Solving Eq. (19) up to terms of order g^2 (in 2nd-order terms, there is no difference between the expansion in powers of the bare coupling constant g and the running coupling constant g_λ , but one should think about the expansion in powers of g_λ , see below and next sections), which includes finding the mass counterterms in the initial condition at $\lambda = \infty$, one obtains H_λ that can change the number of effective particles by 0, 1, or 2. For 2nd-order evaluation of the effective Hamiltonian in the quark-antiquark sector, one only needs the following terms [4]

$$H_\lambda = T_{q\lambda} + T_{g\lambda} + f_\lambda [Y_{qg\lambda} + V_{q\bar{q}\lambda} + Z_{q\bar{q}\lambda}] . \quad (20)$$

$T_{q\lambda}$ and $T_{g\lambda}$ denote the kinetic energy operators for quarks and gluons, respectively. $Y_{qg\lambda}$ denotes the term which causes that effective quarks emit or absorb effective gluons (the letter Y is chosen in the notation because its shape resembles an act of one particle splitting into two, or two particles forming one). $f_\lambda V_{q\bar{q}\lambda}$ is an interaction between quarks due to exchange of gluons with virtuality greater than λ . $f_\lambda Z_{q\bar{q}\lambda}$ is the instantaneous interaction between effective quarks that originates in the instantaneous interaction in the canonical LF Hamiltonian. Details of these terms are listed in Appendix A.

D. Derivation of $H_{Q\bar{Q}\lambda}$

This section explains how one obtains the effective Hamiltonian $H_{Q\bar{Q}\lambda}$ for a heavy quarkonium starting from the eigenvalue problem for the effective Hamiltonian H_λ that reads

$$H_\lambda |P\rangle = E|P\rangle . \quad (21)$$

$|P\rangle$ denotes an eigenstate of the operators P_λ^+ and P_λ^\perp with eigenvalues P^+ and P^\perp (see [40] for an example of RGPEP construction of the whole Poincaré algebra). The eigenvalue has the form $E = (M^2 + P^\perp)^2/P^+$ and by multiplying the equation by P^+ and subtracting P^\perp one obtains an eigenvalue equation for M^2 . $|P\rangle$ is expanded in the effective particle basis as

$$|P\rangle = |Q_\lambda \bar{Q}_\lambda\rangle + |Q_\lambda \bar{Q}_\lambda g_\lambda\rangle + \dots \quad (22)$$

For λ much smaller than m this expansion is dominated by its components with only two heavy quarks because the vertex form factors f_λ in H_λ eliminate the probability of creating components with invariant masses that differ from $2m$ by much more than λ . One may also expect that gluons develop a mass gap in QCD and the components with many gluons are also suppressed. If one neglects sectors with effective gluons entirely, the eigenvalue problem is reduced to

$$[T_{q\lambda} + f_\lambda (V_{q\bar{q}\lambda} + Z_{q\bar{q}\lambda})] |Q_\lambda \bar{Q}_\lambda\rangle = E |Q_\lambda \bar{Q}_\lambda\rangle . \quad (23)$$

But Eq. (21) implies that the $|Q_\lambda \bar{Q}_\lambda g_\lambda\rangle$ component satisfies equation

$$[T_{q\lambda} + T_{g\lambda} + V_{q\bar{q}g\lambda} - E] |Q_\lambda \bar{Q}_\lambda g_\lambda\rangle = -Y_\lambda |Q_\lambda \bar{Q}_\lambda\rangle , \quad (24)$$

and the component with one effective gluon can contribute to the energy of the sector $|Q_\lambda \bar{Q}_\lambda\rangle$ in order g_λ^2 , or $\alpha_\lambda = g_\lambda^2/(4\pi)$, because Y_λ is of order g_λ . $V_{q\bar{q}g\lambda}$ denotes potentials in the three-body sector, including non-abelian potentials that act between the effective gluon and quarks. Additional interactions with sectors that contain four or more effective particles are not indicated. The additional interactions and $V_{q\bar{q}g\lambda}$ are expected to cause a shift in the gluon energy and make the eigenvalue equation differ from a similar one for positronium. In positronium, a state with two or more photons could have the same energy as the state with one photon. In QCD, there exist potential terms that act between gluons and quarks and among gluons themselves that have no counterpart in QED and it is very unlikely that there does not exist some shift in gluon energy that is absent in the case of photons. One can employ an ansatz for the effective gluon mass in the three-body sector to study possible consequences of such shift [4].

The point is that one can study the dynamics of H_λ order by order in g_λ using a scheme of successive approximations that include an ansatz for effects that are extremely small for an infinitesimal g_λ but need to be included to come close to a true solution that is obtained only when the coupling constant takes values comparable with 1. In each successive order one can replace the ansatz terms introduced in a lower order by a true interaction of that lower order but with the coupling constant in them extrapolated to the large physical value [28]. The task of finding the initial ansatz terms that come close to the actual dynamics with large relativistic coupling constant may in principle require a lot of research to complete. Fortunately, the boost-invariant effective particle approach has a useful feature: a lowest-order ansatz that is defined using an effective mass-like term for constituent gluons allows one to easily calculate and eliminate the gluon component and the resulting dynamics of constituent quarks comes out rotationally symmetric and independent of the details of the gluon mass ansatz one makes provided only that the ansatz satisfies some general conditions [4]. In this first approximation, all interactions in the sector $|Q_\lambda \bar{Q}_\lambda g_\lambda\rangle$ are replaced by a function μ^2 of the relative motion of the three constituents.

μ^2 must vanish when the gluon $x \rightarrow 0$. Since the mass ansatz for μ^2 is supposed to model the dominant effect of all the interactions within the three-body sector and with sectors of larger numbers of constituent particles when the coupling constant takes a realistically large value, the first term in the ansatz can be considered to be on the order of 1 in comparison to the terms that depend on the infinitesimal coupling constant used in the formal expansion in RGPEP. The whole eigenvalue problem for H_λ with the ansatz is now reduced to only two coupled equations (we do not indicate λ any more),

$$(T_q + \tilde{T}_g)|Q\bar{Q}g\rangle + Y|Q\bar{Q}\rangle = E|Q\bar{Q}g\rangle, \quad (25)$$

$$Y|Q\bar{Q}g\rangle + [T_q + f(V_{q\bar{q}} + Z_{q\bar{q}})]|Q\bar{Q}\rangle = E|Q\bar{Q}\rangle. \quad (26)$$

The operator \tilde{T}_g is marked with the tilde in order to indicate that the effective gluon mass μ_λ^2 in Eq. (A3) is replaced by the ansatz mass μ^2 in the 3-body sector.

The Hamiltonian $H_{Q\bar{Q}}$ that acts only in the $|Q\bar{Q}\rangle$ sector can now be evaluated as a power series in g using an operator usually denoted by R [41]. In the simplest version, R expresses the 3-body component through the 2-body one, $|Q\bar{Q}g\rangle = R|Q\bar{Q}\rangle$. Note that the sector with an effective gluon is separated from the sector without the effective gluon by a gap in invariant mass. The 2nd-order result is the Hamiltonian whose matrix elements are [4]

$$\begin{aligned} \langle 13 | H_{Q\bar{Q}} | 24 \rangle &= \langle 13 | [T_q + f(V_{q\bar{q}} + Z_{q\bar{q}})] | 24 \rangle + \\ \langle 13 | f Y_{qg} \left[\frac{1/2}{E_{24} - T_q - \tilde{T}_g} + \frac{1/2}{E_{13} - T_q - \tilde{T}_g} \right] f Y_{qg} | 24 \rangle, \end{aligned}$$

where $|ij\rangle$ with i equal 1 or 2 and j equal 3 or 4 are eigenstates of the operator T_q in the $|Q\bar{Q}\rangle$ sector of the Fock space, and E_{ij} are the corresponding eigenvalues. The labeling of states is illustrated in Fig. 7. The basis states are defined as

$$|ij\rangle = b_{\lambda i}^\dagger d_{\lambda j}^\dagger |0\rangle, \quad (27)$$

where b_{λ}^\dagger and d_{λ}^\dagger are creation operators for effective quarks and antiquarks corresponding to the RGPEP width parameter λ . The corresponding eigenvalue is $E_{ij} = (\mathcal{M}_{ij}^2 + P^{\perp 2})/P^+$, where $\mathcal{M}_{ij}^2 = (k_i + k_j)^2$ and the minus components of the four-momenta are evaluated as for free particles with mass m .

In summary, the procedure used here [4] replaces the eigenvalue problem for H_λ by an eigenvalue problem with an ansatz (dots denote operators that couple states with more effective particles than three)

$$[H_\lambda] = \begin{bmatrix} \cdot & \cdot & \cdot \\ \cdot & H_3 & Y \\ \cdot & Y^\dagger & H_2 \end{bmatrix} \rightarrow \begin{bmatrix} T_3 + \mu^2 & Y \\ Y^\dagger & T_2 + V_2 \end{bmatrix}, \quad (28)$$

and then the operation R is used to derive the effective quark Hamiltonian (in a simplified symbolic notation)

$$H_{Q\bar{Q}\lambda} = T_{2\lambda} + V_{2\lambda} + Y_\lambda^\dagger \frac{1}{T_3 + \mu^2} Y_\lambda. \quad (29)$$

The procedure should not be confused with a conventional Tamm-Dancoff approach to quantum field theory. The quantum particle degrees of freedom that are obtained from RGPEP are not the bare quanta of local canonical theory, see [42], and the effective particles obey rules of the LF dynamics with a vacuum that is simple to work with. Moreover, the effective particles interact through terms like Y_λ that contain vertex form factors whose width has interpretation of the size of the effective particles in strong interactions (the particles cannot emit or absorb any quanta with greater invariant mass changes than λ). At the same time, λ also plays the role of the RGPEP parameter in the differential equations that control the evolution of operators from the canonical ones at $\lambda = \infty$ to the effective ones that can be used in a relativistic computation of bound states when λ is lowered to the scale of the hadronic masses. The relativistic nature of the procedure is reflected by the possibility to construct all generators of the Poincaré group at the scale λ at which one wishes to solve the eigenvalue problem for H_λ itself [40].

Although the eigenvalue problem for heavy quarkonia in QCD with explicit inclusion of the sector with 3 effective particles has not been studied in detail yet, it is important to state here that the ansatz scheme dictates in this case the replacement

$$\begin{bmatrix} \cdot & \cdot & \cdot & \cdot \\ \cdot & H_4 & Y_1 & Y_2 \\ \cdot & Y_1^\dagger & H_3 & Y \\ \cdot & Y_2^\dagger & Y^\dagger & H_2 \end{bmatrix} \rightarrow \begin{bmatrix} T_4 + \mu^2 & Y_1 & Y_2 \\ Y_1^\dagger & H_3 & Y \\ Y_2^\dagger & Y^\dagger & H_2 \end{bmatrix} \quad (30)$$

and subsequent application of R to the desired order. These steps appear to resemble the LF Tamm-Dancoff scheme with sector-dependent counterterms proposed by Perry, Harindranath, and Wilson [43]. The conceptual difference is that in the Perry-Harindranath-Wilson scheme the elimination of sectors occurs within a Hamiltonian eigenvalue problem with large cutoffs and the ultraviolet renormalization issue is a part of the problem, leading to Wilson's triangle of renormalization with a vast and virtually unknown space of relativistic quantum operators. In the scheme used here [4], the ultraviolet renormalization group procedure is completed long before one tackles the eigenvalue problem and introduces an ansatz at the scale λ near the magnitude of invariant masses that characterize observables. The principles of extracting a small and computer-soluble eigenvalue problem from an eigenvalue problem of infinite size, such that the results obtained from a small problem can represent solutions to the infinite problem, will be further explained below.

Finally, it should be stressed that the mass ansatz has the structure [4]

$$\mu_{ansatz}^2 = [1 - \alpha_\lambda^2/\alpha_s^2] \mu^2, \quad (31)$$

where α_s denotes the large, relativistic coupling constant that the effective coupling α_λ is supposed to reach as a

result of extrapolation from the infinitesimal values used in the perturbative solution of the equations of RGPEP. This structure ensures that in the lowest-order approximate expressions obtained through expansion in powers of α_λ , only the first term counts,

$$\mu_{ansatz}^2 = \mu^2. \quad (32)$$

This term is order 1. But when one increases the order of included terms and extrapolates to $\alpha_\lambda = \alpha_s$, the ansatz is removed and one has a chance to recover a true solution of the initial theory with increasing accuracy. Comparisons of results obtained from expansions in successive orders, and use of better extrapolation techniques than through a plain power series, will hopefully indicate if the procedure can converge on a well-defined dynamical picture. One should compare the initial approximate theories with experiment and find out if the coupling constants required to explain data can be small enough to pursue the chain of calculations based on the weak-coupling expansion. Results of this study suggest that at least for heavy quarkonia the required coupling constant in LF QCD is considerably smaller than 1, see below.

E. Eigenvalue equation for $H_{Q\bar{Q}\lambda}$

The eigenvalue equation for $H_{Q\bar{Q}\lambda}$ has the form

$$H_{Q\bar{Q}\lambda}|Q_\lambda\bar{Q}_\lambda\rangle = \frac{M^2 + P^{\perp 2}}{P^+}|Q_\lambda\bar{Q}_\lambda\rangle. \quad (33)$$

The eigenstates are written as (see Appendices A and B for details of the notation, we drop λ)

$$|M, P^+, P^\perp\rangle = \int [ij] \tilde{\delta} P^+ \frac{\bar{u}_i \Psi_{ij} v_j}{-4m^2} |ij\rangle. \quad (34)$$

The eigenstate wave function can be written in the form that exhibits its covariance under 7 kinematical LF Poincaré transformations,

$$\Psi_{ij} = \sum_{s_i s_j} \Psi_{s_i s_j}(\vec{k}_{ij}) u_{k_i, s_i} \bar{v}_{k_j, s_j}, \quad (35)$$

$$\Psi_{s_i s_j}(\vec{k}_{ij}) = \bar{u}_{\vec{k}_{ij}, s_i} \Psi_{CMFij}(\vec{k}_{ij}) v_{-\vec{k}_{ij}, s_j}, \quad (36)$$

where $\Psi_{CMFij}(\vec{k}_{ij})$ denotes the wave function that depends on the relative three-momentum of quarks in their CMF, assuming their masses are just m . The indices s_i and s_j denote projections of spin on z -axis. Spinors u_{k_i, s_i} and v_{k_j, s_j} are obtained using LF boost matrix ($\Lambda^\pm = \gamma^0 \gamma^\pm / 2$)

$$B(k, m) = \frac{1}{\sqrt{k^+ m}} [k^+ \Lambda^+ + \Lambda^- (m + k^\perp \alpha^\perp)] \quad (37)$$

acting on the spinors at rest, $u_{0,s}$ and $v_{0,s}$, in the reference frame in which the bound state calculation is carried

out and where the four-momentum of the bound state has components P^+ , P^\perp , and $P^- = (M^2 + p^\perp 2) / P^+$, M being the eigenvalue that one wants to calculate. Spinors $u_{\vec{k}_{ij}, s_i}$ and $v_{-\vec{k}_{ij}, s_j}$ are obtained by “boosting” spinors at rest in the CMF of the constituent fermions along their relative three-momentum. An additional spatial rotation is applied in the CMF before the latter boost is applied in order to build a spin basis in which one obtains explicit rotational symmetry of spin-dependent interactions in the leading approximation. The additional rotation is the same as the well-known Melosch transformation [44, 45]. Details of our notation for momentum variables, spinors, and boost matrices, are explained in Appendices B and C.

Eq. (33) implies the eigenvalue equation for the wave function,

$$0 = \left[\frac{\kappa_{13}^{\perp 2} + m_\lambda^2}{x_1 x_3} + \frac{m_{Y1}^2}{x_1} + \frac{m_{Y3}^2}{x_3} - M^2 \right] \Psi_{s_1 s_3}(\vec{k}_{13}) - \frac{\frac{4}{3} g^2}{16\pi^3} \int \frac{dx_2 d^2 \kappa_{24}^\perp}{x_2 x_4} \sum_{s_2 s_4} v_\lambda(13, 24) \Psi_{s_2 s_4}(\vec{k}_{24}), \quad (38)$$

in which the mass-like terms m_{Y1}^2 and m_{Y3}^2 result from the self-interaction of effective quarks through emission and re-absorption of effective gluons, and $v_\lambda(13, 24)$ results from the exchange of the effective gluon between the two quarks. The ultraviolet-finite part of the mass counterterm in the effective quark mass m_λ^2 is so adjusted (using a single quark eigenvalue problem) that at $\lambda = \lambda_0$ one obtains [4]

$$\left[\frac{\kappa_{13}^{\perp 2} + m^2}{x_1 x_3} + \frac{\delta m_1^2}{x_1} + \frac{\delta m_3^2}{x_3} - M^2 \right] \Psi_{s_1 s_3}(\vec{k}_{13}) - \frac{\frac{4}{3} g^2}{16\pi^3} \int \frac{dx_2 d^2 \kappa_{24}^\perp}{x_2 x_4} \sum_{s_2 s_4} v_0(13, 24) \Psi_{s_2 s_4}(\vec{k}_{24}) = 0, \quad (39)$$

where

$$v_0(13, 24) = -A g_{\mu\nu} j_{12}^\mu \bar{j}_{43}^\nu + B \frac{j_{12}^+ \bar{j}_{43}^+}{P^+ 2}, \quad (40)$$

and δm_1^2 , δm_3^2 , A , B , and other symbols, are explained in detail in Appendix B.

III. LEADING APPROXIMATION

The RGPEP result of Eq. (39) is further analyzed as a typical window Hamiltonian eigenvalue problem of the kind studied in detail in the case of a generic matrix model with asymptotic freedom and a bound state [46, 47, 48]. The model is soluble exactly and provides a relatively well-understood pattern to follow in the case of QCD with one heavy flavor. Earlier LF studies, based on coupling coherence [49, 50, 51, 52, 53], did not use

a boost-invariant concept of effective particles, were carried out in a frame of reference nearly at rest with respect to the CMF of the quarkonium, and employed a logarithmically confining potential that was obtained in the quark-antiquark sector neglecting all other sectors. Those studies pioneered an attack on the bound-state problem in LF QCD along the path discussed by Perry [50, 51], including elements of the method outlined in Wilson et al. [28], such as the absolute cutoffs on momentum variables (especially k^+) in the Fourier analysis of field variables in position space, or similarity RG procedure for Hamiltonians. One of the key issues of the LF approach is how to obtain rotational symmetry and the initial studies had to struggle with the issue, in addition to the issue of construction of counterterms that restore boost symmetry violated by cutoffs on absolute momentum variables. The RGPEP procedure used here leads in its simplest version to a boost-invariant and rotationally symmetric spectrum of meson masses.

A. Coupling constant in the window

Construction of a window eigenvalue problem begins with a selection of a set of basis states with kinetic energies (actually, free invariant masses) in a certain range that is also called a window, for brevity. The size of this range should be larger than the width λ_0 which appears in the form factors f in H_{λ_0} .

The next step is to evaluate matrix elements of H_{λ_0} in the selected window of basis states. These matrix elements form a matrix W of the window Hamiltonian whose non-perturbative diagonalization is to produce the bound state of interest.

Typically, if the energy range (the word “energy” should be replaced by the words “invariant mass” almost everywhere in this paper, but the reader is expected to be more familiar with the word energy than invariant mass in reference to the quantum dynamical concepts that count here and we use the word energy in order to avoid confusion due to the lack of familiarity with the LF form of quantum Hamiltonian dynamics) in the window Hamiltonian matrix W is sufficiently larger than λ_0 , the middle eigenvalues of the window are independent of the window boundaries and they match the eigenvalues of the full H_{λ_0} . The latter eigenvalues are equal to the exact eigenvalues of the initial Hamiltonian H if the RGPEP procedure is carried out exactly. The additional virtue of lessons from Ref. [48], beyond showing that an asymptotically free model can be solved using a window, is that one can also evaluate the matrix elements of W in perturbation theory, as if the coupling constant was extremely small. One sets the coupling constant to a realistically large value when one solves the non-perturbative eigenvalue problem for W .

The point is that a few low orders in RGPEP calculation of W may lead to a good approximation (reaching better accuracy than 10% for the bound-state eigenval-

ues already when W is calculated in second order) if one properly chooses λ_0 in order to work with a small number of basis states (small means small enough so that they can be handled using computers) and if one adjusts the coupling constant in the window to the chosen λ_0 . λ_0 should be near the scale of invariant masses that dominate in the binding mechanism. The coupling constant is defined through the value of a specific matrix element in the window. It is adjusted by comparison of the spectrum of W with data (in [48], the role of data is played by the known exact spectrum). The main result of the matrix model (studied so far up to 6th order, or 5 loop integrals) is that when the coupling constant in the window W is adjusted so that one middle eigenvalue of W matches the corresponding exact solution then also other middle eigenvalues of W approximate the corresponding exact solutions.

In a theory as complex as QCD, the RGPEP calculations of window Hamiltonians beyond 2nd order will require a lot of work. Completion of the 4th order calculation is important for determination of the accuracy one can achieve using window Hamiltonians in QCD. Apart from the plain perturbative expansion, one may eventually take advantage of the idea of coupling coherence [49], reformulated for the use in RGPEP. However, when additional flavors of quarks are included and their masses are lowered toward small values known in the standard model, one may have to deal with an infrared limit cycle [54] (and universality that may apply in that case [55], instead of the asymptotic freedom structure known in the ultraviolet). But in the case of heavy quarks, i.e., when the quark mass is formally very large in comparison to Λ_{QCD} , the value of the coupling constant required in the window may be small and no complications possible for light quarks are expected to occur.

B. Heavy quark limit

In a formal analysis of QCD with one heavy flavor, the quark mass m can be much larger than λ_0 and the latter much larger than Λ_{QCD} . In these circumstances, the perturbative coupling constant corresponding to λ_0 is small and the relative motion of quarks in the sector $|Q\bar{Q}\rangle$ is limited by the form factors f of width λ_0 . This means that the dominant relative momenta of quarks in mesons are small in comparison to m . (One should observe that the process of extrapolation of the window to a large value of the coupling constant corresponds to the increase in the value of Λ_{QCD} ; at a phenomenologically useful value of $\alpha_0 = \alpha_{\lambda_0}$, one may have to work with λ_0 that is no longer very small in comparison to m). Formally, in the limit of large m , the dominant dynamical effects in the window eigenvalue Eq. (39) with $\lambda_0 \ll m$ can be analyzed using a non-relativistic approximation for the relative motion of quarks. The arbitrary motion of the meson as a whole can be exactly separated from the relative motion of the constituent quarks because the

RGPEP is invariant under the LF boosts. However, approaching the IMF, one will observe that the differences between absolute values of momenta of the quantum constituents extend to much larger values than the mass of the entire meson. The differences correspond to some fixed range of Feynman x around 1/2. But every fixed value of a difference in x implies that the corresponding quark momenta in the IMF differ by amounts infinitely larger than any fixed mass parameter.

The non-relativistic approximation is formally validated by the condition that $\lambda_0 \ll m$, and that the interaction terms are growing not faster than a polynomial of kinetic energy (invariant mass) and cannot overcome the exponential falloff of the form factors f for changes of invariant masses that are larger than λ_0 . Thus, in order to use the non-relativistic expansion, one has to keep in place the exponential form factors f that provide the convergence - these form factors determine the size of the window in momentum space and one cannot expand the exponential function in a series. What can be expanded are the arguments of the exponential functions, the perturbative factors that appear in RGPEP in addition to the form factors, spin dependent factors in interaction vertices, and relativistic measure of integration over relative momenta of quarks. The accuracy of results of diagonalization of the window W_{λ_0} will depend on the choice for the form factor function f and, especially, on the optimization factors that are critical for the convergence of the perturbative evaluation of H_{λ_0} in 4th order [47, 48]. The optimization factors were considered in the case of heavy quarkonia elsewhere [56]. The study described here was carried out using f of the generic type exemplified in Eq. (17). Every form factor considered here is the same exponential function of the square of a difference of squares of invariant masses of the effective particles in interaction.

When Eq. (39) is written in the non-relativistic approximation for the RGPEP, spin, and integration measure factors, the limit of small coupling exhibits scaling property similar to the Schrödinger equation for positronium. The scaling in RGPEP is described at the beginning of Appendix B. The scaling implies that the quark eigenvalue problem is dominated by the relative momenta on the order of strong Bohr momentum,

$$k_B = \frac{4}{3} \alpha_0 \frac{m}{2}, \quad (41)$$

which is the quark analog of $\alpha m_e/2$ in positronium in QED. This scale emerges from the window eigenvalue condition independently of the value of λ_0 as long as λ_0 is sufficiently large in comparison to k_B . In other words, the eigenvalues M^2 depend mainly on the value of α_{λ_0} and not on the value of λ_0 itself when λ_0 is much larger than k_B . We do not answer here the question of how large λ_0 must be in comparison to k_B in order to obtain results that are sensitive to λ_0 practically only through the value of α_0 , or to what extent this lack of direct sensitivity to λ_0 itself is obtained for realistic values of

α_0 and λ_0 . A study of such issues has been done before in a model based on Yukawa theory [42, 57].

In a formal analysis of the non-relativistic expansion for infinitesimal coupling constant α_0 , one can assume that

$$\lambda_0 = \lambda_m \frac{m}{2}, \quad (42)$$

$$\lambda_m = \left(\frac{4}{3} \alpha_0 \right)^{0.5+\epsilon} \lambda_p. \quad (43)$$

λ_0 is much smaller than $m/2$ when λ_p is on the order of 1. The two parameters λ_p and ϵ are useful in separating different terms in the complex, spin-dependent interactions that otherwise do not occur clearly ordered in size. The particular choice of the power $0.5 + \epsilon$ follows from how the form factors f limit momentum transfers in vertices. The most interesting case is ϵ close to 0 (see below). At the same time, k_B is much smaller than λ_0 as long as $0 < \epsilon < 0.5$. In the formal analysis, k_B is considered much larger than Λ_{QCD} when one evaluates the window W_{λ_0} using RGPEP. But when one extrapolates the coupling constant in the window to realistic values, a realistically large value of Λ_{QCD} is introduced, instead of an infinitesimally small one. The ansatz for the gluon mass gap corresponds to the scale of the realistic Λ_{QCD} .

Note that the formally introduced relationship between λ_0 and α_0 does not mean that one replaces the true RGPEP dependence of α_0 on λ_0 by an artificial one. All that is done is to introduce a parameterization of an unknown infinitesimal value of α_0 at a single value of λ_0 ; the parameters λ_m , λ_p , and ϵ , remain free to change while k_B stays always much smaller than λ_0 . After the scaling picture is described using this parameterization and identifying terms that scale with different powers of α_0 , one can look for the values of m and λ_m for which the scaling picture extrapolated to large values of the coupling constant is useful phenomenologically. At that point one identifies the realistic values of α_0 and λ_0 . All one obtains this way is an approximate picture for heavy quarkonium dynamics that can serve as a starting point for a systematic calculation of corrections using RGPEP.

C. Scaling of different factors

The scaling expansion of RGPEP factors A and B that occur in the potential $v_0(13, 24)$ in Eq. (39), in terms of powers of α_0 (we shall omit the subscript 0 below whenever it is irrelevant to the context) is given in Eqs. (B43) and (B44). The first terms in the scaling expansion that provide the leading approximation are

$$A \simeq -f \frac{1}{q^2} + ff \frac{1}{q^2} \frac{\mu^2}{q^2 + \mu^2}, \quad (44)$$

$$B \simeq 4m^2 ff \frac{1}{q_z^2} \frac{\mu^2}{q^2 + \mu^2}. \quad (45)$$

The symbol q denotes the three-momentum transferred between quarks. The self-interaction terms δm^2 contain the same function B in their integrands.

The RGPEP factors ff behave as

$$ff \simeq \exp \left[-2 \left(\frac{mq^2}{q_z \lambda^2} \right)^2 \right]. \quad (46)$$

Using definitions of Eqs. (B25) and (B26) for momenta and (42) and (43) for λ_0 , one obtains

$$ff \simeq \exp \left\{ - \frac{8p^2}{\left[\left(\frac{4}{3}\alpha \right)^\epsilon \lambda_p \right]^4 \cos^2 \theta} \right\}, \quad (47)$$

where q_z was replaced by $q \cos \theta$ and θ is the angle between \vec{q} and z -axis. For small α , the form factors are not zero only for small p , and, in fact, only for vanishingly small p when the angle θ between \vec{p} and z -axis approaches $\pi/2$. Unless there exists a large contribution in the region of small p , especially near $\theta \sim \pi/2$, from other factors in the potential, the factor ff is equivalent to zero when α is near 0 in the scaling analysis. But B can be large for $\theta \rightarrow \pi/2$ due to q_z^2 in denominator. This singular behavior originates in the instantaneous LF potential due to gauge coupling between colored particles. One has to find the result that survives in the limit of small α in the presence of the singularity. The factor regulating the singularity at $q_z = 0$ is provided by the ansatz function μ^2 . When one combines the terms with ff in the self-interactions δm^2 and in A and B in the gluon exchange potential, the net result is a spherically symmetric and spin-independent harmonic oscillator potential whose spring constant is no longer sensitive to the mass ansatz μ^2 under quite general assumptions [4]. The oscillator frequency is

$$\omega = \sqrt{\frac{4}{3} \frac{\alpha}{\pi}} \lambda \left(\frac{\lambda}{m} \right)^2 \left(\frac{\pi}{1152} \right)^{1/4}, \quad (48)$$

and the corresponding spring constant, $k = m\omega^2/2$, leads in the dimensionless Schrödinger equation in variables \vec{p}_{ij} , defined in Eq. (B25), to the oscillator term that scales like $\alpha^{6\epsilon}$ and becomes independent of α when $\epsilon \rightarrow 0$, see Eq. (50) below. The oscillator potential is independent of the quark spins.

According to Eq. (40), all spin effects in the leading approximation originate from the current factors that multiply the term $-f/q^2$ in A in Eq. (44). The leading spin effects can be identified using the same scaling analysis. In the scaling analysis for infinitesimal α , spin-dependent terms are α^2 times smaller than the spin-independent terms. Therefore, one can also try to include corrections order α^2 that do not depend on spin. However, the spin-independent correction terms order α^4 that emerge from the scaling expansion based on only 2nd-order RGPEP violate rotational symmetry and are expected to cancel out or get corrected when the window is calculated in 4th-order RGPEP. Since the spin factors have

distinct origin (quark current factors that are specific to QCD) than the generic RGPEP factors (the same in all field theories) and momentum space integration measure (universal in relativistic particle physics), the structure of interaction kernels that one encounters in the scaling equation (in addition to the spin-independent harmonic oscillator term) can be written as (the factor α^2 in front is not included)

$$\mathcal{V} = f \left(\frac{4\pi}{p^2} + \alpha^2 R \right) (1 + \alpha^2 S)(1 + \alpha^2 M), \quad (49)$$

where R refers to the RGPEP factors, S to spin, and M to measure.

We drop the term R because it depends on the z -axis and can only be corrected in the 4th order calculation for RGPEP factors. In the 2nd-order RGPEP factors analyzed here, the correction R is given by the term c in Eq. (B43) and when one averages this term over the direction of the z -axis, it vanishes. Nevertheless, one should remember that a genuine 4th-order calculation of H_λ may produce corrections of the type R that will change the radial dependence of the potential from the Coulomb shape to a different one.

In order to identify the leading spin effects, we combine the spin and measure corrections to the factor $1 + \alpha^2(S + M)$ and write it shortly as $1 + BF$, where BF stands for Breit-Fermi terms. The point is that one can observe cancellation between S and M factors and the remaining terms produce a rotationally symmetric spin-dependent terms after one introduces an additional turn of the spin basis that is described in Appendix C.

D. Structure of the eigenvalue problem

Finally, using dimensionless variables \vec{p}_{13} and \vec{p}_{24} (Fig. 7 illustrates the labeling of the momentum variables) defined in Eqs. (B25) and (B26), one arrives at the following eigenvalue equation for the spin-dependent 2×2 matrix wave function ϕ , defined in Eqs. (D4) and (D5):

$$0 = [\vec{p}_{13}^2 - k_p \Delta_{p_{13}} - x] \phi(\vec{p}_{13}) - 2 \int \frac{d^3 p_{24}}{(2\pi)^3} \mathcal{V} \phi(\vec{p}_{24}), \quad (50)$$

$$\mathcal{V} = f \frac{4\pi}{p^2} (1 + BF), \quad (51)$$

$$f = \exp \left\{ - \left[\left(\frac{4}{3}\alpha \right)^{1-2\epsilon} \frac{p_{13}^2 - p_{24}^2}{\lambda_p^2} \right]^2 \right\}, \quad (52)$$

$$k_p = \frac{1}{\sqrt{1152\pi}} \frac{\lambda_p^6}{16} \left(\frac{4}{3}\alpha \right)^{6\epsilon}. \quad (53)$$

In the limit $\alpha \rightarrow 0$ in the above result, the eigenvalues x tend to $-1/n^2$ with natural n (the Balmer series). One obtains meson masses by evaluating the eigenvalues x for

realistic values of α and using the formula

$$M = 2m \sqrt{1+x \left(\frac{2}{3}\alpha\right)^2}. \quad (54)$$

This relationship between the eigenvalues x and meson masses exists in the LF Hamiltonian dynamics because the dynamics is invariant with respect to boosts.

The fact that a mass-gap ansatz for gluons leads to an oscillator-like interaction term, which respects rotational symmetry already in the 2nd-order analysis, in which $\mu^2 \sim 1$, does not seem accidental. The result is almost independent of all details of the ansatz because q^2 is limited by the form factors ff in the function B of Eq. (45) to so small values that the ratio $\mu^2/(q^2 + \mu^2)$ is practically 1 for any reasonable ansatz. In addition, it seems not excluded that the same result comes out also as a part of the genuine 4th-order calculation. In the 4th-order calculation, the part of the ansatz for μ^2 that is order 1 may cancel out in the window W with large α . Looking at Eqs. (29) and (29), one can see that the ansatz term order 1 in the three-body sector is eliminated in 4th-order RGPEP calculation when one includes the three-body sector in the non-perturbative window dynamics. If instead one uses the perturbative operation R to further reduce the window to the two-body quark-antiquark sector only, the cancellation of the ansatz begins in 6th-order calculation. There can exist cancellations for large coupling that cannot be easily foreseen. But even if the ansatz is not introduced at all, some shift of the three-body invariant mass, say μ_1^2 , will emerge from QCD interactions of formal order α in the 3-body sector and this is how the actual gap may show up for the first time. When one proceeds to the scaling analysis of functions analogous to A and B in Eqs. (44) and (45), the new shift will be of order α if it is proportional to m^2 , of order $\alpha^{3/2}$ if it is proportional to $m\lambda$, and of order α^2 if it is proportional to λ^2 . But the momentum transfer squared, q^2 , is of order α^2 and it may continue to be formally much smaller than or comparable to μ_1^2 in the scaling limit of small α . The form factor f limits $|\vec{q}|$ to values on the order of $(|t|/2) \lambda_p^2 (4\alpha/3)^{2\epsilon} k_B$, where $t = \cos\theta$ and θ is the angle between the momentum of the effective gluon and the z -axis. The terms that lead to the harmonic force originate from the singular behavior of $q_z^{-2} \sim 1/t^2$ when $t \rightarrow 0$. But one can still neglect $q^2 \sim t^2 \alpha^{2+4\epsilon}$ in comparison to $\mu_1^2 \sim \alpha^n t^{1+\delta_\mu}$ with $n = 1$ and $3/2$, and even for $n = 2$ the result of integration may be close to the one obtainable when q^2 is neglected in comparison to μ_1^2 , cf. [4]. Also, if the effective mass ansatz is just a first term in the expansion of the gluon gap in powers of the gluon momentum squared, which corresponds to the case with $\mu^2 \sim q^2 t^\delta$ in the limit of small t [4], the scaling applies in the same way and leads to the same oscillator result [4]. So, if some mass gap shows up in order α in the 3-body sector, as one expects it to happen in QCD, the results of Eqs. (44) and (45) may still be valid.

IV. SPIN EFFECTS

Spin effects are caused by the Breit-Fermi terms, BF in Eq. (51), that originate from the product of currents $j_{12}^\mu \bar{j}_{43}^\mu$ in v_0 in Eq. (40). In the leading approximation, v_0 is displayed in Eq. (D1). The spinors u_{k_i, s_i} and v_{k_j, s_j} in the currents originate from the canonical LF Hamiltonian of QCD and they are related by boosts \mathcal{L}_{ij} described in Appendix C to the spinors $u_{\tilde{k}_{ij}, s_i}$ and $v_{-\tilde{k}_{ij}, s_j}$ that are introduced in the definition of the CMF wave function $\Psi_{CMFij}(\tilde{k}_{ij})$ in Eq. (36).

It is shown in Appendix D that the BF terms in Eq. (51) are

$$BF\phi = \frac{\alpha^2}{9} \left[3(p_{24}^2 + p_{13}^2) a - \vec{p} \vec{\sigma} \vec{b} \vec{\sigma} \vec{p} \vec{\sigma} + 3\vec{p}_{13} \vec{\sigma} \vec{p}_{24} \vec{\sigma} \vec{b} \vec{\sigma} + 3\vec{b} \vec{\sigma} \vec{p}_{24} \vec{\sigma} \vec{p}_{13} \vec{\sigma} \right], \quad (55)$$

where ϕ denotes the 2×2 matrix wave function $\phi = a + \vec{b} \vec{\sigma}$ and \vec{p} is the difference between \vec{p}_{13} and \vec{p}_{24} . An alternative form of the same result,

$$BF\phi = \frac{\alpha^2}{3} (p_{24}^2 + p_{13}^2) a + \frac{\alpha^2}{9} \left[(4\vec{p}_{13} \vec{p}_{24} + p_{13}^2 + p_{24}^2) \vec{b} \vec{\sigma} + \vec{b} (8\vec{p}_{24} - 2\vec{p}_{13}) \vec{p}_{13} \vec{\sigma} - \vec{b} (4\vec{p}_{13} + 2\vec{p}_{24}) \vec{p}_{24} \vec{\sigma} \right], \quad (56)$$

shows that the singlet wave function a and the triplet wave function \vec{b} are not coupled and describe different eigenstates.

The resulting eigenvalue equations for different mesons are listed in subsections below. These equations are boost-invariant and describe the relative motion of two heavy quarks no matter how fast the whole quarkonium is moving, which is also reflected in Eq. (54) that differs from a non-relativistic expression for energy of a slowly moving object, $E = M + E_B + P^2/(2M)$, where the binding energy E_B is given by some Schrödinger equation. In order to obtain a state of a moving quarkonium, one has to insert the wave function ϕ into Eq. (34), using Eqs. (35), (36), (D4), and (D5), all of which are relativistic. Note that the eigenvalue equations in the subsections below lead to non-local interactions at short distances if one introduces position variables canonically coupled with the relative three-momenta of quarks defined here in a boost invariant way. The reason for non-locality is that the interactions contain the form factors, f , that depend on the differences of invariant masses before and after an interaction. One should remember that although the equations in the next subsection look deceptively simple and like in non-relativistic models, they describe wave functions that from the models' point of view formally correspond to different frames of reference for different values of the modulus of the relative three-momenta, see Appendices.

Note also that the interaction terms in the equations listed below include potentials that in the absence of the form factors f would produce three-dimensional Dirac δ -functions in the position space representation. The δ -functions would lead to ultraviolet divergences. But the form factors f smear the δ -functions and render finite results. Nevertheless, the terms with the smeared δ -functions are not weak when α is extrapolated to values on the order of 1 and they contribute to significant spin effects for states that involve significant s -wave components.

A. Mesons η_c and η_b

In this case, $\vec{b} = 0$ and the eigenvalue equation for $\phi(\vec{p}_{ij}) = a_{ij}/p_{ij}$ takes the form

$$0 = [\vec{p}_{13}^2 - k_p \Delta_{p_{13}} - x] \frac{a_{13}}{2p_{13}} - \int \frac{d^3 p_{24}}{(2\pi)^3} \mathcal{V} \frac{a_{24}}{p_{24}}, \quad (57)$$

where

$$\mathcal{V} = f \frac{4\pi}{p^2} \left[1 + \frac{\alpha^2}{3} (p_{24}^2 + p_{13}^2) \right]. \quad (58)$$

The orbital angular momentum is zero and the integration over angles (see Appendix E) produces a one-dimensional integral equation

$$0 = h_{sosc} a_{13} - \frac{2}{\pi} \int_0^\infty dp_{24} f p_{13} p_{24} \mathcal{W} a_{24}, \quad (59)$$

with

$$\mathcal{W} = \left[1 + \frac{\alpha^2}{3} (p_{24}^2 + p_{13}^2) \right] J_0, \quad (60)$$

where the function J_0 is given in Appendix E.

$$h_{sosc} = p_{13}^2 - k_p \partial_{13}^2 - x \quad (61)$$

is introduced as a generic notation for the s -wave harmonic oscillator terms in the mass eigenvalue equations for all mesons.

B. Mesons J/Ψ and Υ

In this case $a = 0$ and the eigenvalue equation describes a function $\phi(\vec{p}_{ij}) = \vec{b}_{ij} \vec{\sigma}$, where

$$b_{13}^k = \left[\delta^{kl} \frac{S_{13}}{p_{13}} + \frac{1}{\sqrt{2}} \left(\delta^{kl} - 3 \frac{p_{13}^k p_{13}^l}{p_{13}^2} \right) \frac{D_{13}}{p_{13}} \right] s^l, \quad (62)$$

and \vec{s} is a polarization vector of a massive meson of spin 1. The s -wave wave function S and d -wave wave function

D satisfy two coupled equations

$$\begin{aligned} 0 = & \begin{bmatrix} h_{sosc}, & 0 \\ 0, & h_{sosc} + k_p \frac{6}{p_{13}^2} \end{bmatrix} \begin{bmatrix} S_{13} \\ D_{13} \end{bmatrix} \\ & - \frac{2}{\pi} \int_0^\infty dp_{24} f p_{13} p_{24} \begin{bmatrix} \mathcal{W}_{ss}, & \mathcal{W}_{sd} \\ \mathcal{W}_{ds}, & \mathcal{W}_{dd} \end{bmatrix} \begin{bmatrix} S_{24} \\ D_{24} \end{bmatrix}, \end{aligned} \quad (63)$$

where

$$\mathcal{W}_{ss} = J_0 + \frac{\alpha^2}{3} [(p_{13}^2 + p_{24}^2) J_0 - 16/9], \quad (64)$$

$$\mathcal{W}_{sd} = \frac{\alpha^2}{3} [p_{13}^2 (J_2 - J_0) + 4/3] \frac{\sqrt{2}}{3}, \quad (65)$$

$$\mathcal{W}_{ds} = \frac{\alpha^2}{3} [p_{24}^2 (J_2 - J_0) + 4/3] \frac{\sqrt{2}}{3}, \quad (66)$$

$$\mathcal{W}_{dd} = J_2 + (J_2 - J_0)/2 \quad (67)$$

$$+ \frac{\alpha^2}{3} \{ (p_{13}^2 + p_{24}^2) [J_0 - (J_2 - J_0)/6] - 20/9 \},$$

and the functions J_0 and J_2 are given in Appendix E.

C. Mesons χ_{c0} and χ_{b0}

Here $a = 0$ and the eigenvalue equation for $\phi(\vec{p}_{ij}) = b_{ij} \vec{p}_{ij} \vec{\sigma}/p_{ij}^2$ takes the form

$$0 = \left(h_{sosc} + k_p \frac{2}{p_{13}^2} \right) b_{13} - \frac{2}{\pi} \int_0^\infty dp_{24} f p_{13} p_{24} \mathcal{W} b_{24}, \quad (68)$$

where (see Appendix E)

$$\mathcal{W} = J_1 + \frac{\alpha^2}{9} [p_{13} p_{24} 8 J_0 - (p_{13}^2 + p_{24}^2) J_1]. \quad (69)$$

D. Mesons χ_{c1} or χ_{b1}

Here again $a = 0$ and the radial eigenvalue equation for $\phi(\vec{p}_{ij}) = b_{ij} \vec{s} \times \vec{p}_{ij} \vec{\sigma}/p_{ij}^2$ takes the form

$$0 = \left(h_{sosc} + k_p \frac{2}{p_{13}^2} \right) b_{13} - \frac{2}{\pi} \int_0^\infty dp_{24} f p_{13} p_{24} \mathcal{W} b_{24}, \quad (70)$$

where

$$\mathcal{W} = J_1 + \frac{\alpha^2}{9} [2 p_{13} p_{24} (J_0 + J_2) + (p_{13}^2 + p_{24}^2) J_1]. \quad (71)$$

E. Mesons χ_{c2} or χ_{b2}

In this case also $a = 0$ and the eigenvalue equation is for

$$\phi_{13} = \mathcal{S}_n \frac{p_{13}^i}{p_{13}} s_n^{ij} \sigma^j \frac{P_{13}}{p_{13}}$$

$$+ \mathcal{S}_n \sqrt{\frac{2}{7}} \frac{p_{13}^i}{p_{13}} \left[s_n^{ij} - \frac{5}{2} \delta^{ij} \frac{p_{13}^k}{p_{13}} s_n^{kl} \frac{p_{13}^l}{p_{13}} \right] \sigma^j \frac{F_{13}}{p_{13}}, \quad (72)$$

where s_n^{ij} with $n = 1, 2, \dots, 5$ are symmetric traceless 3×3 matrices, \mathcal{S}_n is the corresponding polarization five-vector for a massive meson with spin 2 (the sum over n from 1 to 5 is indicated only by the repeated subscript n). The p -wave wave function P_{13} and the f -wave wave function F_{13} satisfy two coupled equations

$$0 = \begin{bmatrix} h_{sosc} + k_p \frac{2}{p_{13}^2}, & 0 \\ 0, & h_{sosc} + k_p \frac{12}{p_{13}^2} \end{bmatrix} \begin{bmatrix} P_{13} \\ F_{13} \end{bmatrix} - \frac{2}{\pi} \int_0^\infty dp_{24} f p_{13} p_{24} \begin{bmatrix} \mathcal{W}_{pp}, & \mathcal{W}_{pf} \\ \mathcal{W}_{fp}, & \mathcal{W}_{ff} \end{bmatrix} \begin{bmatrix} P_{24} \\ F_{24} \end{bmatrix}, \quad (73)$$

where

$$\begin{aligned} \mathcal{W}_{pp} &= J_1 + \alpha^2 p_{13} p_{24} \frac{14}{45} (3J_2 - J_0) \\ &+ \alpha^2 (p_{24}^2 + p_{13}^2) \frac{1}{45} J_1, \end{aligned} \quad (74)$$

$$\begin{aligned} \mathcal{W}_{pf} &= -\alpha^2 p_{13} p_{24} \frac{2\sqrt{6}}{45} (3J_2 - J_0) \\ &+ \alpha^2 \frac{\sqrt{6}}{45} [p_{24}^2 2J_1 + p_{13}^2 (5J_3 - 3J_1)], \end{aligned} \quad (75)$$

$$\begin{aligned} \mathcal{W}_{fp} &= -\alpha^2 p_{24} p_{13} \frac{2\sqrt{6}}{45} (3J_2 - J_0) \\ &+ \alpha^2 \frac{\sqrt{6}}{45} [p_{13}^2 2J_1 + p_{24}^2 (5J_3 - 3J_1)], \end{aligned} \quad (76)$$

$$\begin{aligned} \mathcal{W}_{ff} &= (5J_3 - 3J_1)/2 + \alpha^2 p_{13} p_{24} \frac{16}{45} (3J_2 - J_0) \\ &- \alpha^2 (p_{13}^2 + p_{24}^2) \frac{1}{90} (5J_3 - 3J_1), \end{aligned} \quad (77)$$

and the functions J_0 , J_1 , J_2 , and J_3 , are given in Appendix E.

F. Singlets with $J = 2$, or 1D_2

In this case $\vec{b}_{ij} = 0$ and

$$\phi_{13} = \mathcal{S}_n \frac{a_{13}}{p_{13}} \frac{p_{13}^i s_n^{ij} p_{13}^j}{p_{13}^2}. \quad (78)$$

The eigenvalue equation for the function a reads

$$0 = \left[h_{sosc} + k_p \frac{6}{p_{13}^2} \right] a_{13} - \frac{2}{\pi} \int_0^\infty dp_{24} f p_{13} p_{24} \mathcal{W} a_{24}, \quad (79)$$

where

$$\mathcal{W} = \left[1 + \frac{\alpha^2}{3} (p_{24}^2 + p_{13}^2) \right] \left(\frac{3}{2} J_2 - \frac{1}{2} J_0 \right). \quad (80)$$

G. Triplets with $J = 2$, or 3D_2

In this case $a = 0$ and

$$\phi_{13} = \mathcal{S}_n \frac{b_{13}}{p_{13}} \frac{p_{13}^i s_n^{ij} (\vec{p}_{13} \times \vec{\sigma})^j}{p_{13}^2}. \quad (81)$$

The eigenvalue equation takes the form

$$0 = \left[h_{sosc} + k_p \frac{6}{p_{13}^2} \right] b_{13} - \frac{2}{\pi} \int dp_{24} f p_{13} p_{24} \mathcal{W} b_{24}, \quad (82)$$

with

$$\begin{aligned} \mathcal{W} &= \left[1 + \frac{\alpha^2}{9} (p_{13}^2 + p_{24}^2) \right] \left(\frac{3}{2} J_2 - \frac{1}{2} J_0 \right) \\ &+ \frac{4\alpha^2}{9} p_{13} p_{24} J_3. \end{aligned} \quad (83)$$

V. MASSES AND WAVE FUNCTIONS

This section describes examples that illustrate to what extent the simplest version of the RGPEP approach can reproduce masses of the known $b\bar{b}$ and $c\bar{c}$ mesons and how the corresponding wave functions may depend on the relative momentum of the quarks.

A. Coupling constant and quark mass

One potentially valid way to determine the coupling constant α_λ and quark mass m_λ in H_λ at $\lambda = \lambda_0$ is to evolve their values as functions of λ using RGPEP from the region of large λ , say $\lambda = \lambda_1$, where their values may be adjusted to observables that are minimally sensitive to the non-perturbative mechanism of binding of quarks and gluons. For such observables, the adjustment could be made using a perturbative expansion for the S -matrix for quarks and gluons using H_{λ_1} in the femtouniverse [58]. Although a precisely defined calculation including bound states as asymptotic states does not exist yet in the RGPEP approach to QCD, some patterns expected to occur in such calculation have already been studied. For example, the RGPEP evolution that starts at λ_1 must be extended down to λ_0 comparable to the meson mass and to reach that far one has to deal with issues of convergence that require optimization of details of the method [48]. It is also known [35] that the differential equations of RGPEP that describe the evolution of the operator H_λ (not the S -matrix) produce in third-order perturbation theory in QCD the coupling constant that evolves with λ according to the formula

$$\alpha_0 = \frac{\alpha_{M_Z}}{1 + [\alpha_{M_Z}/(6\pi)] (11N_C - 2n_f) \ln(\lambda_0/M_Z)}, \quad (84)$$

which matches the well-known formula for the running coupling constant in the original Lagrangian calculus for

the QCD action [59, 60]. Here, α_{M_Z} is the coupling constant in H_{λ_1} with $\lambda_1 = M_Z$, $M_Z = 92.1$ GeV is the mass of the Z -boson, $N_C = 3$ is the number of colors and n_f is the number of flavors (the theory analyzed here has $n_f = 1$). Thus, as soon as one estimates the value of the coupling constant at one value of λ in the boost-invariant Hamiltonian approach, such as $\lambda_1 = M_Z$, its size at other values of λ is in principle known in the entire region, in which the perturbative RGPEP calculus for the Hamiltonians can be accurate.

For example, if one assumes that $\alpha_{M_Z} \sim 0.12$ [29], one obtains $\alpha_0 \sim 0.326$ at $\lambda_0 \sim 3.7$ GeV (for $n_f = 6$, one would obtain $\alpha_0 \sim 0.21$). However, if one uses the same formula in a strict expansion in powers of α_{M_Z} to third order only, one obtains a result that is about 30% smaller than 0.326. The reason is that Eq. (84) predicts an increasingly rapid growth of the coupling constant when λ decreases. But the perturbative formula is replaced by a non-perturbative one for λ near the bound-state mass, and this can be studied in detail using models [46, 47]. By analogy with the models, one may expect a finite but rapid transition of α from the increasing to a decreasing function of λ in the region where the binding mechanism dominates dynamics, smoothing the discontinuity present in the perturbative formula for α when its denominator tends to zero. Therefore, a low-order expansion in powers of α_{M_Z} is not useful. But it is useful to expand the operator H_{λ_0} in powers of α_0 . The operator coefficients of this expansion can be found assuming that α_0 is infinitesimally small [48]. The same coefficients can be used for evaluating H_{λ_0} when λ_0 is small and α_0 is comparable with 1. Finding a precise formula for α_0 in terms of α_{λ_1} for realistic values of the coupling constants may require sophisticated high-order RGPEP calculations. If the precise value of α_0 cannot be easily calculated in a low-order perturbation theory, one can seek values of α_0 that may correspond to the available bound-state data and then incorporate the resulting picture in a new perturbation theory around the first approximation found that way. At the present stage of development, one can only verify if the simplest version of the boost-invariant Hamiltonian approach can reproduce known masses of heavy quarkonia when the coupling constant α_0 is allowed to take values on the order of 1.

Less is known about the quark mass m as a function of λ , and what values of m_{λ_0} one should expect in H_{λ_0} . Technically, the mass parameter is specified as the perturbative eigenvalue of H_{λ_0} for one-quark states [4]. Therefore, one can expect that the mass should be close to the pole mass [29], which is about 10% larger than the quark mass in the minimal subtraction scheme for bottom quarks. One may expect for $b\bar{b}$ mesons that $m = m_{\lambda_0} \sim 4.5$ GeV to 5 GeV.

Thus, although in principle the boost-invariant Hamiltonian approach appears able to cover the whole range of energy scales accessible experimentally in the case of heavy quarkonia, to correlate high-energy perturbative results in the femtouniverse with the description of bind-

ing of quarks and gluons at the scale of b or c quark masses, one needs higher-order calculations than studied here in the simplest version of the approach. In the simplest version, one can only find out if there exist choices for the parameters α and m at λ_0 on the order of the quark masses that can produce spectra of masses of the quarkonia with reasonable accuracy. Since one expects $\alpha \sim 1/3$, “reasonable” means here that the masses should be reproducible with accuracy on the order of 1/3 or perhaps 1/10 of the largest splittings between states with neighboring quantum numbers. The latter are on the order of 500 MeV and this means that matching data with accuracy on the order of 50 MeV would be quite good in the simplest version if the required α and m for such matching are close to the values established from other considerations.

In principle, masses of two mesons are sufficient to fix the values of α and m as functions of λ near λ_0 . The question is which two masses one should use. That the choice is not obvious and that there is a need for a good choice is a consequence of the fact that in approximate calculations all masses are calculated with theoretical errors that are not known and if one uses two masses that are obtained with a large theoretical error then results for all other masses will be obtained with large errors. Experience with exactly solvable models dictates that the most accurate procedure should be to choose the masses in the middle of the spectrum of the window Hamiltonian [42, 48]. Let us consider the example of $b\bar{b}$ mesons. The most rational choice is to use masses of two p -wave mesons $\chi_1(1P)$ and $\chi_1(2P)$. Their masses lie in the middle of the window spectrum. The high-energy boundary of the window corresponds to short distance dynamics, i.e., the most tightly bound states, having the smallest masses. The low-energy boundary corresponds to long distance dynamics, i.e., the states with largest masses. The mesons $\chi_1(1P)$ and $\chi_1(2P)$ are not very sensitive to the short distance dynamics and thus also not very sensitive to the unknown term $\alpha^2 R$ in the potential of Eq. (49), because quarks in these mesons are pushed out from the region of small relative distances by the centrifugal barrier with $l = 1$. One expects that RGPEP of 4th-order will produce terms $\alpha^2 R$ that correspond in position space to functions like $\delta^3(\vec{r})$ or $1/r^3$. Such functions are known to occur in effective potentials in standard dynamics in atomic calculations in QED when one includes effects due to the exchange of two photons, vertex corrections, and self-interactions order α^2 [23]. Thus, selecting mesons $\chi_1(1P)$ and $\chi_1(2P)$ that have $l = 1$, one has a chance to avoid theoretical errors due to the current lack of knowledge of the terms $\alpha^2 R$ in LF QCD. At the same time, the masses of mesons $\chi_1(1P)$ and $\chi_1(2P)$ are most probably less sensitive to the quark-antiquark long-distance dynamics than the masses of states with $l = 2$ or 3. At long inter-quark distances, the harmonic oscillator potential is expected to lose accuracy because the simplest approximation does not take into account effective gluons that may be created when quarks move

far away from each other. For example, one effective gluon could actively participate in the non-perturbative dynamics of states with masses that exceed the middle eigenvalues of the window Hamiltonian by more than 1 GeV, which is an estimate of the magnitude of mass of an effective gluon at the scale λ_0 . The estimate indicates that one should probably fit parameters α and m in the simplest approximation to meson masses that do not exceed the middle masses by more than about 1 GeV, and the mesons $\chi_1(1P)$ and $\chi_1(2P)$ lie in this range.

TABLE I: Qualitative illustration of results of the simplest approximate approach to heavy quarkonia in the case of masses of $b\bar{b}$ mesons (in MeV). The second column is obtained using the quark mass $m = 4856.92$ MeV and coupling constant $\alpha = 0.32595$ for $\lambda = 3697.67$ MeV when one demands that the masses of mesons $\chi_1(1P)$ and $\chi_1(2P)$ are reproduced using an auxiliary interpolation procedure described in the text, which is employed only to increase speed of numerical estimates in this illustration and is accurate to a few MeV. The corresponding oscillator parameters are $\omega = 182.16$ MeV and $k_p = 0.157722$. The third column quotes experimental data with accuracy to 1 MeV and the fourth column displays the difference. The fifth column shows precise numerical results obtained from the same dynamical equations for the same values of m , α , and λ , but without errors introduced by the auxiliary interpolation procedure.

meson	interpolation	experiment [29]	difference	precise
$\Upsilon 10865$	10725	10865	-140	10729.7
$\Upsilon 10580$	10464	10580	-116	10466.9
$\Upsilon 3S$	10382	10355	27	10385.2
$\chi_2 2P$	10276	10269	7	10278.5
$\chi_1 2P$	10256	10256	0	10258.0
$\chi_0 2P$	10226	10232	-6	10228.1
$\Upsilon 2S$	10012	10023	-11	10013.8
$\chi_2 1P$	9912	9912	-1	9913.3
$\chi_1 1P$	9893	9893	0	9894.2
$\chi_0 1P$	9865	9859	5	9865.5
$\Upsilon 1S$	9551	9460	91	9551.8
$\eta_b 1S$	9510	9300	210	9510.8

An example of results one obtains by fitting masses of $b\bar{b}$ mesons $\chi_1(1P)$ and $\chi_1(2P)$ for $\lambda_0 = 3697.67$ MeV is given in Table I. The coupling constant and mass required to obtain the two masses at this λ_0 are $\alpha = 0.32595$ and $m = 4856.92$ MeV, in a good qualitative agreement with expectations (see Eq. (84) and the discussion that follows it). The large number of digits in these numbers is a numerical effect due to the precision of experimental data and does not reflect the accuracy of the Hamiltonian approach to QCD in its simplest version with only $|Q\bar{Q}\rangle$ sector, which is presumably much worse. The value of λ_0 chosen in this example lies in the middle of a small range of size of about 200 MeV in which one can vary λ_0 and numerically reproduce the same known values of the two meson masses with accuracy better than 1 ppm by varying the parameters α and m as functions of λ_0 . Table I shows that a whole set of masses in the middle of the window spectrum is also close to data when the

two selected masses are. The masses near the edges of the window, most sensitive to the theoretical errors of the simplest version, deviate from data by more than the masses in the middle of the window spectrum do, but the magnitude of these deviations is not absurdly large.

Results in Table I were obtained in a sequence of steps that need to be explained. The key difficulty is that the masses can be determined only numerically, and the integrals that determine matrix elements of the window Hamiltonians depend simultaneously and in nontrivial way on α , m , and λ . The complication is caused mainly by the form factors f , which eliminate the possibility of analytic integrations using the oscillator basis functions. The numerical evaluation of the matrix elements of window Hamiltonians takes time. The time required for evaluation of one matrix element on a good laptop is on the order of a second, and one needs on the order of a thousand matrix elements to obtain accuracy of four digits for masses of mesons that result from diagonalization of the window matrix. One would have to carry out very long computations to find suitable α and m for any given choice of λ_0 if one were computing matrix elements always a new for every change in the parameters. Instead, one can evaluate eigenvalues x in Eqs. (59) to (82) using parameters that lie on discrete points of a grid in the parameter space. The parameter k_p is more convenient than λ itself. Then one can interpolate between the grid points in order to find approximate eigenvalues for a continuum of parameters α and m for a whole range of values of λ_0 in the region covered by the grid. Such interpolation produces quickly results of precision better than 10^{-3} . The interpolating functions allow one to identify the values of α and m that reproduce the same masses of $\chi_1(1P)$ and $\chi_1(2P)$ for different values of λ_0 very efficiently even though the eigenvalues are less precise than 1 MeV. Results of the interpolation are given in Table I in the second column, marked “interpolation.” Precisely evaluated masses for the parameters selected using the interpolation are given in the fifth column in Table I.

The example given in Table I shows that even in its simplest version the Hamiltonian approach can lead to phenomenologically reasonable results for the masses of $b\bar{b}$ mesons. But the example does not provide information about how large is the range of parameters for which the simplest version of the Hamiltonian approach can match the masses of known heavy quarkonia. This issue is taken up using examples in the remaining parts of this section.

B. Masses of $b\bar{b}$ mesons

In order to obtain qualitative information about the distance between the simplest version of LF QCD and data for masses of $b\bar{b}$ mesons, one can consider two different fits of α and m .

One fit is focused on the middle of the mass spectrum of known mesons. Instead of fixing two selected meson masses and checking how others are reproduced as it was

done in the previous subsection, one finds a minimum of deviation of the computed masses from data as function of α and m assuming different λ_0 and this is done for 7 masses in the middle of the experimentally known spectrum. Results of this fit are denoted in Table II as “fit to middle.” They are shown graphically in Fig. 1. Variation of the obtained spectrum with λ_0 when one keeps any two of the 7 masses fixed, or rather the degree of absence of such variation, is not further studied in this and the next subsection.

TABLE II: Masses of $b\bar{b}$ mesons (in MeV). The third column results from the fit of the coupling constant α and quark mass m at the indicated optimal value of λ to 7 middle masses of known $b\bar{b}$ mesons, i.e., masses of $\chi_0(1P)$, $\chi_1(1P)$, $\chi_2(1P)$, $\Upsilon(2S)$, $\chi_0(2P)$, $\chi_1(2P)$, $\chi_2(2P)$, and this fit implies the oscillator parameters $\omega = 184.62$ MeV and $k_p = 0.26667$. The fourth column results from the fit to masses of all 12 mesons $\eta(1S)$, $\Upsilon(1S)$, $\chi_0(1P)$, $\chi_1(1P)$, $\chi_2(1P)$, $\Upsilon(2S)$, $\chi_0(2P)$, $\chi_1(2P)$, $\chi_2(2P)$, Υ^3D_1 (estimated as similar to D_2), $\Upsilon(3S)$, $\Upsilon 10580(S4)$, and the corresponding oscillator parameters are $\omega = 147.11$ MeV and $k_p = 0.016667$. Question marks regarding D states are explained in the text.

	experiment [29]	fit to middle	fit to all
λ [MeV]	—	3779.8	3252.3
m [MeV]	—	4835.9	4979.7
α	—	0.28839	0.50738
$\Upsilon 10580$	10580 ± 3.5	10734	10629
Υ^3D_1	—	10461	10446
$\Upsilon 3S$	10355.2 ± 0.5	10389	10329
$\chi_2 2P$	10268.5 ± 0.72	10273	10272
$\chi_1 2P$	10255.5 ± 0.72	10256	10241
$\chi_0 2P$	10232.5 ± 0.9	10231	10194
Υ^1D_2	$10161.1? \pm 2.2$	—	10172
Υ^3D_2	$10161.1? \pm 2.2$	—	10169
Υ^1D_1	—	10115	10154
$\Upsilon 2S$	10023.3 ± 0.31	10018	9991
$\chi_2 1P$	9912.21 ± 0.57	9907	9943
$\chi_1 1P$	9892.78 ± 0.57	9892	9908
$\chi_0 1P$	9859.44 ± 0.73	9869	9849
$\Upsilon 1S$	9460.3 ± 0.26	9574	9448
$\eta_b 1S$	9300.6 ± 10	9542	9359

The other fit is focused on checking how many of the experimentally known meson masses can be explained in the simplest version of LF QCD, and how accurately. The second fit includes masses of all 12 well-established mesons [29] with decay widths significantly smaller than 100 MeV. A decay width comparable with 100 MeV is considered an indicator of relevance of processes that the simplest approximate version of LF QCD cannot describe. The second fit is denoted in Table II as “fit to all.” The results are shown graphically in Fig. 2.

A separate comment is required concerning the D states (d -waves) in Table II. One such state is known experimentally [29], most probably having total $J=2$. This state is included in the table in order to illustrate what happens in the simplest version of LF QCD concerning d -wave mesons. All D states, whether one con-

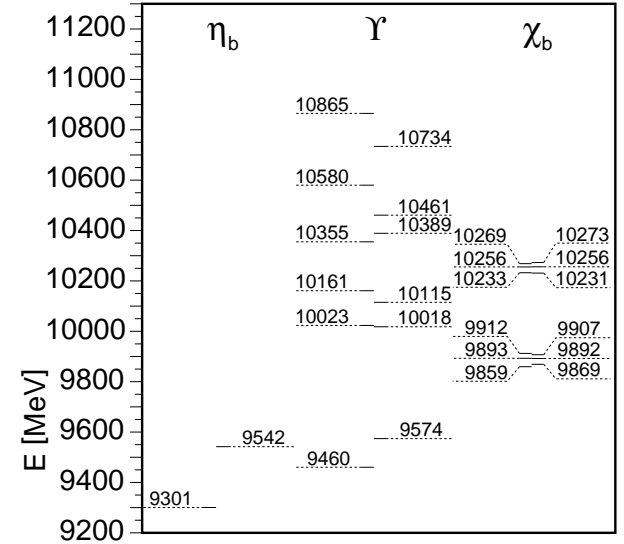


FIG. 1: Illustration of masses in the 3rd column in Table II. The left thick bars in each of the three columns indicate data and right thick bars results of computation. The theory mass 10461 MeV corresponds to a state dominated by the d -wave, apparently not easy to identify experimentally [29].

siders singlets or triplets, or $J = 1$, are expected in other approaches to have similar masses [61, 62]. The same happens in LF QCD. In Table II, the state Υ^1D_1 is known only in theory, and masses of both states Υ^1D_2 and Υ^3D_1 are near the one experimentally known mass of 10161 MeV for the D -meson that presumably has $J = 2$. The excited triplet state Υ^3D_1 is not known experimen-

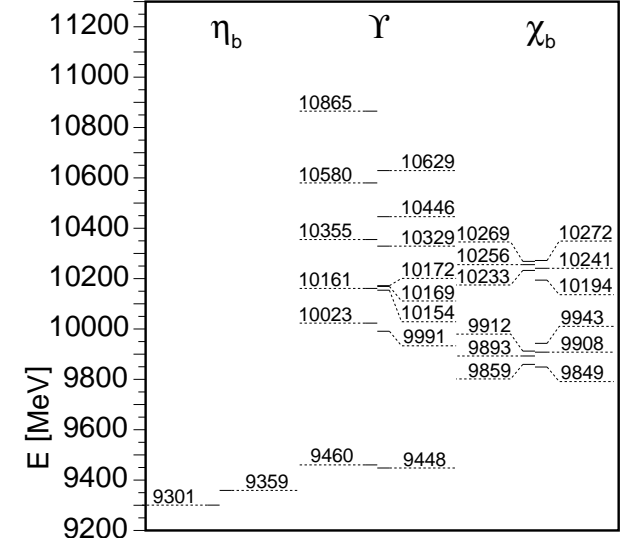


FIG. 2: Illustration of masses in the 4th column in Table II. The left thick bars in each of the three columns indicate data and right thick bars results of computation. The theory D -state mass changes by only a few MeV, to 10446 MeV, when one changes “fit to middle” to “fit to all.”

tally but comes out of the calculation as dominated by its d -wave component. In Fig. 1 for $b\bar{b}$ mesons, the known mass of 10161 MeV is shown in comparison with the theoretical mass of the Υ state dominated by d -wave, and, in Fig. 2, it is shown in comparison with all three theoretical results for D states with $J = 2$ and $J = 1$.

The range of coupling constants α_0 and quark masses m_0 for which the Hamiltonians $H_{Q\bar{Q}\lambda_0}$ can match the data for $b\bar{b}$ mesons, as illustrated in Tables I and II, and in Figs. 1 and 2, is summarized using these examples in Table III (subscript 0 is omitted). Note that the fit to

TABLE III: Parameters in H_{λ_0} for $b\bar{b}$ mesons.

parameter	χ_1	7 middle	all 12
λ [MeV]	3697.67	3779.8	3252.3
m [MeV]	4856.92	4835.9	4979.7
α	0.32595	0.28839	0.50738

all 12 meson masses points to the much larger coupling constant and quark mass at considerably smaller λ_0 than in the two similar cases with fits to 7 or only 2 middle mesons. This feature most probably emerges because the term $\alpha^2 R$ in the radial factor $1 + \alpha^2 R$ in Eq. (49) is set to 0 in the simplest version of the approach. Splittings between s -wave mesons, including the η_b and Υ family, are sensitive to the short-distance dynamics that depends on the term $\alpha^2 R$. Calculation of the term $\alpha^2 R$ requires full 4th-order RGPEP analysis. In the absence of $\alpha^2 R$, one can nearly reproduce masses of the s -wave states at the price of increasing α and m . However, it is clear that the 4th-order calculation of the term $\alpha^2 R$ must be carried out in order to narrow the range of possible values of α and m .

C. Masses of $c\bar{c}$ mesons

Masses of $c\bar{c}$ mesons can be studied in the simplest version of the Hamiltonian approach analogously to the case of $b\bar{b}$ mesons discussed in the previous subsection. Table IV shows results of two fits: to 3 middle masses in the known spectrum, and to all 11 masses of well-established mesons with small decay widths. Masses of two theoretical D states with $J = 2$ can in principle be compared with the one experimentally known mass of 3836 MeV for a meson whose $J = 2$ needs confirmation [29]. Fig. 3 illustrates the results for $c\bar{c}$ mesons obtained from the fit to the three middle masses in the window (the third column in Table IV), the D -mesons with $J = 2$ are not illustrated. In Fig. 4, illustrating results from the fit to the masses of all 11 $c\bar{c}$ mesons (the fourth column in Table IV), all three states with d -waves; the triplet $J = 1$ state corresponding to $\psi 3770$, the triplet state, and the singlet state with $J = 2$, are indicated.

Table V shows examples of parameters that fit masses of $c\bar{c}$ mesons, in comparison to the examples of parameters from Table III that fit masses of $b\bar{b}$ mesons. It is

TABLE IV: Masses of $c\bar{c}$ mesons (in MeV). The third column results from the fit of the coupling constant α and quark mass m at the indicated optimal value of λ to only 3 middle masses of $c\bar{c}$ mesons, i.e., masses of $\chi_0(1P)$, $\chi_1(1P)$, $\chi_2(1P)$, and this fit implies the oscillator parameters $\omega = 284.93$ MeV and $k_p = 3.0642$. The fourth column results from the fit to masses of all 11 mesons $\eta(1S)$, $J/\psi(1S)$, $\chi_0(1P)$, $\chi_1(1P)$, $\chi_2(1P)$, $\eta(1S)$, $\psi(2S)$, $\psi 3770$, $\psi 4040$, $\psi 4159$, $\psi 4415$, and the corresponding oscillator parameters are $\omega = 278.72$ MeV and $k_p = 1.3396$. Question marks regarding D states are explained in the text.

meson	experiment [29]	fit to middle	fit to all
λ [MeV]	—	1990.0	1934.2
m [MeV]	—	1553.3	1577.4
α	—	0.34335	0.41443
$\psi 4415$	4415 ± 6	4505	4462
$\psi 4159$	4159 ± 20	4178	4152
$\psi 4040$	4040 ± 10	4122	4083
1D_2	$3836? \pm 13$	—	3801
3D_2	$3836? \pm 13$	—	3793
$\psi 3770$	3770 ± 2.4	3773	3756
$\psi 2S$	3686.093 ± 0.034	3698	3662
$\eta_c 2S$	3638 ± 5	3619	3557
$\chi_2 1P$	3556.26 ± 0.11	3560	3551
$\chi_1 1P$	3510.59 ± 0.1	3507	3481
$\chi_0 1P$	3415.16 ± 0.35	3412	3340
$J/\psi 1S$	3096.916 ± 0.011	3199	3156
$\eta_c 1S$	2980.4 ± 1.2	3111	3024

plausible that the anomalously large result of $\alpha \sim 0.5$ for bottom quarks merely indicates that a fit to all masses can push parameters toward explanation of the large s -wave splittings at the expense of theoretical consistency of the approach. It is expected that α in $b\bar{b}$ mesons should be smaller than in $c\bar{c}$ mesons, in correspondence with the

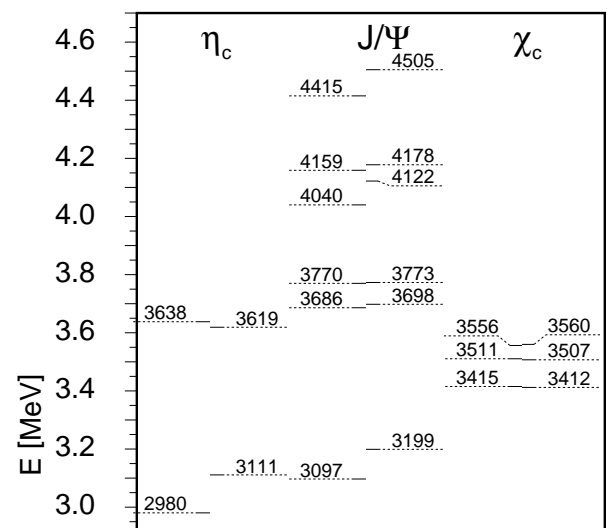


FIG. 3: Illustration of masses in the 3rd column in Table IV. The left thick bars in each of the three columns indicate data and right thick bars results of computation.

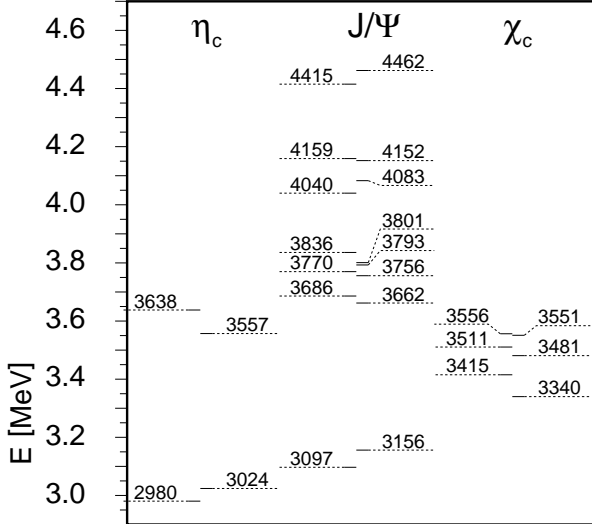


FIG. 4: Illustration of masses in the 4th column in Table IV. The left thick bars in each of the three columns indicate data and right thick bars results of computation.

increase of λ_0 . Calculation of the term $\alpha^2 R$ in 4th-order RGPEP should clarify the situation considerably.

At this point, one can observe that the Hamiltonians $H_{Q\bar{Q}\lambda_0}$ obtained for heavy quarkonia in the simplest version of LF QCD seem to explain the tendency of potential models to prefer larger values of the coupling constant and quark masses than indicated by results based on perturbative QCD [29]. Namely, when one forces a single non-relativistic Hamiltonian with a Coulomb potential at short distances and some confining potential at large distances to fit data for masses of many mesons, instead of only the middle ones in the window where a simple potential model can be justified, the strong-interaction relativistic effects at short distances are not well described. Similarly, at large distances between quarks, a simple potential model cannot reproduce effects due to interactions that involve gluons “in the air.” The parameters of potential models have to increase artificially in order to keep reproducing the smallest and largest masses of known mesons.

A characteristic feature in Table V is that the quark mass varies slowly with changes of λ_0 while the coupling constant varies relatively quickly. The width parameter λ occurs in third power in the oscillator frequency, ω , in Eq. (48). Therefore, there is a possibility to keep a

TABLE V: Examples of parameters in H_{λ_0} that fit masses of $c\bar{c}$ mesons, compared with the examples of parameters that fit masses of $b\bar{b}$ mesons.

parameter	$b\bar{b}$ middle	$b\bar{b}$ all	$c\bar{c}$ middle	$c\bar{c}$ all
λ_0 [MeV]	3779.8	3252.3	1990.0	1934.2
m [MeV]	4835.9	4979.7	1553.3	1577.4
α	0.28839	0.50738	0.34335	0.41443

whole set of meson masses approximately constant when λ_0 is changed a little by a considerably larger percentage of change in α , while an a priori possible compensating change of the quark mass cannot be large because the overall scale of masses is dictated by Eq. (54). The eigenvalues x are negative for the smallest-mass mesons and positive for the other mesons. Thus, variation of the quark mass is limited by the requirement of preserving the relativistic structure of the spectrum in Eq. (54).

Finally, one should stress that the adjustment of α and m at $\lambda = \lambda_0$, which includes a choice of λ_0 , does not provide a check on the renormalization group variation of the parameters α and m with λ beyond the qualitative statement of agreement with expectations regarding the magnitudes of the parameters. In order to study the renormalization group structure, one would have to consider a plausible choice of α and m at certain λ_0 , evolve the values of α and m in RGPEP for H_λ to other values of λ , and solve the eigenvalue problems for different values of λ . One would need to include the 4th-order RGPEP to begin with and also perform non-perturbative computations of the spectra of window Hamiltonians with more than one Fock sector built from effective particles. Such studies require many elements far beyond the simplest version of the Hamiltonian approach that is discussed here.

D. Wave functions

An important aspect of the LF Hamiltonian dynamics is that it provides wave functions of bound states. This aspect can be discussed already in the simplest version of the approach that is considered here. The discussion that follows is focused on the examples of mesons J/ψ and the ground state of Υ . These states contain s -wave and d -wave wave functions that are invariant under boosts. Section II E explains how the states of quarkonia are constructed using these functions.

The J/ψ and Υ wave functions have the structure indicated in Eq. (62). The s -wave wave function is denoted by S , and the d -wave wave function by D . Both are functions of the relative momentum \vec{k} of the two effective quarks only through its length, $k = |\vec{k}|$. This is a consequence of that the wave functions S and D depend on the invariant mass squared of the two quarks, $\mathcal{M}^2 = 4(m^2 + k^2)$. The relative momentum \vec{k} shares many properties with the momentum-space variable typically introduced in non-relativistic potential models, but one has to remember that the variable \vec{k} appears in QCD according to the rules of LF dynamics.

The wave functions S and D are shown in Figs. 5 and 6 in four versions, two for the ground state of Υ and two for J/ψ . Two versions per meson are obtained using the two choices of parameters α and m that are given in Tables II and IV. Numerical values of the wave functions can be read from the tables give in Appendix G.

It is visible that the d -wave component is much larger

in size in the charm case than in the bottom case, al-

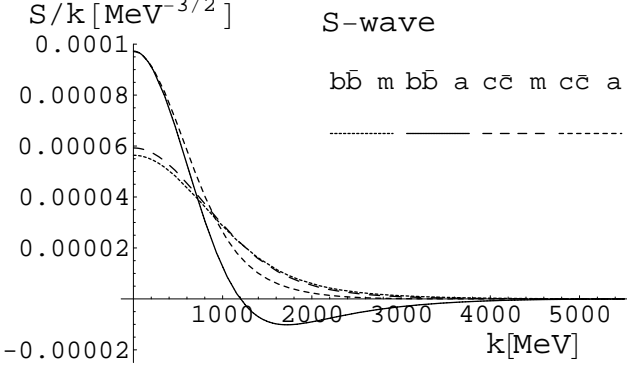


FIG. 5: Four examples of *s*-wave wave functions in $b\bar{b}$ and $c\bar{c}$ mesons. Two curves labeled $b\bar{b}$ correspond to the ground state of Υ and the two curves labeled $c\bar{c}$ correspond to J/ψ . The curves are presented in two versions that correspond to the two sets of parameters α and m shown in Tables II and IV. One set was adjusted to masses in the middle of the known spectrum, and the other one to masses of all known mesons with small widths. The label "m" refers to "middle" and the label "a" to "all."

though the *s*-wave components are similar in both cases at small relative momenta. This result can be attributed to much more relativistic relative motion of quarks in J/ψ than in Υ . Relativistic motion leads to enhancement of spin-dependent interactions that mix the *d*-wave component with the *s*-wave component.

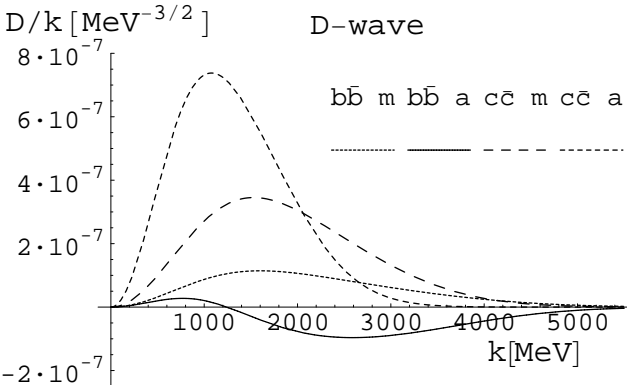


FIG. 6: Four examples of *d*-wave wave functions in the ground state of Υ and in J/ψ . The curves are labeled in the same way as in Fig. 5.

The most prominent feature displayed by the wave functions is their high sensitivity to the size of the coupling constant α , see Table V. The increase of α when one passes from the fit to the middle of the window spectra to the fit to all mesons with small decay widths, is related to the development of a node in the Υ wave functions, for $\alpha \sim 0.5$. A tendency for the same effect is displayed also in the wave functions of J/ψ , but $\alpha \sim 0.4$ seems insufficient to create a clear node. Thus, one can see that

the potential models that tend to explain the entire spectrum of masses have to deal with a complex dynamical situation that strongly depends on the coupling constant in the range of interest.

A comment is in order regarding decay widths of the mesons. In the leading approximation, the leptonic decay amplitudes are proportional to the *s*-wave wave functions at the origin in position space (integrals of the wave functions in momentum space). But Fig. 5 shows that the integrals of the wave functions may be sensitive to the size of α . One needs to find the function α_λ in the range of widths λ that is suitable for diagonalization of perturbatively-evaluated window Hamiltonians in QCD: masses of mesons alone indicate a range from 0.2 to 0.5. There is little doubt that the leptonic decay widths in the Hamiltonian approach to QCD will be qualitatively similar to the widths obtainable in potential models. On the other hand, inclusion of the term $\alpha^2 R$ in the effective potential and corresponding self-interactions in $H_{Q\bar{Q}\lambda}$, in a calculation similar to the simplest version discussed here, and further evaluation of the gluonic components in the effective-particle Fock-space basis in the eigenvalue problem for H_λ , may provide quantitative insight into effects not accessible in potential models. These effects may influence the leptonic decay rates and need to be evaluated in order to precisely compare the theory with data including the decay rates. The point is that such studies appear feasible using the boost-invariant Hamiltonian approach to QCD.

VI. CONCLUSION

The simplest version of computation of masses of heavy quarkonia in QCD with one flavor of quarks that is described in this article, suggests that the boost-invariant Hamiltonian approach [4] offers a feasible path to extended studies of quark and gluon dynamics in the light-front Fock space. One can use creation and annihilation operators for effective particles in order to explicitly construct the states of heavy quarkonia. The approach produces an approximate constituent picture that is relativistic and usable for description of fast-moving mesons. Masses of the mesons are reproduced in the simplest version reasonably well for reasonable values of the coupling constant, α , and quark mass, m . In the simplest version, the short-distance high-energy effects and large-distance gluon dynamics are not fully described. Therefore, the simplest approach describes most accurately only a small set of meson masses that lie in the middle of the spectra of small effective Hamiltonians called "windows," see Section III.

The Hamiltonian calculus produces the boost-invariant wave functions that describe heavy quarkonia in terms of their virtual effective-particle components in the LF Fock space. In principle, these wave functions not only provide a relativistic quantum image of a single hadron, but they also can be used in description of decays, production,

and scattering of the quarkonia using QCD. Although the cases discussed here concern only $b\bar{b}$ and $c\bar{c}$ systems, the extension to the case of unequal masses, such as $b\bar{c}$ or $c\bar{b}$ mesons, requires only that instead of the relative momentum variable \vec{k} used here (see Appendix B) one uses the momentum variable defined in analogous way by the relations

$$k^\perp = \kappa^\perp, \quad (85)$$

$$\begin{aligned} \sqrt{m_1^2 + \vec{k}^2} + \sqrt{m_2^2 + \vec{k}^2} \\ = \sqrt{\frac{m_1^2 + \kappa^\perp 2}{x_1} + \frac{m_2^2 + \kappa^\perp 2}{x_2}}. \end{aligned} \quad (86)$$

Associated momentum-space techniques to handle two- and three-particle systems with different masses in the context of studies of the bound-state structure or decay are sufficiently advanced in the LF approach to handle states that contain quarks and gluons [63]. It is also known that the gluon mass ansatz technique works reasonably well in the case of gluonium [64]. Thus, it seems plausible that the case of different quark masses may be treated with explicit inclusion of the quark-antiquark-gluon sector. Knowing the corresponding wave functions, one can attempt to describe a host of new exclusive or semiexclusive processes that involve heavy quarkonia in arbitrary motion.

The formalism of LF dynamics in quantum field theory involves a choice of an axis in space, especially in gauge theories such as QCD, where one has to make a choice of gauge depending on that axis. Therefore, the rotational symmetry of the theory is not explicit in the LF Hamiltonian formalism. Most of the expressions one encounters depend on the distinguished axis. It is reassuring that the LF Hamiltonian approach to heavy quarkonia produces in its simplest version developed here explicit expressions for bound-state spectra in which masses are exactly arranged in multiplets corresponding to the total angular momentum (meson spin) $J = 0$, $J = 1$, and $J = 2$, and the wave functions of the corresponding states are classifiable as waves s , p , d , and f . Nevertheless, the complete expressions for the wave functions contain additional relativistic factors that are entirely outside the scope of non-relativistic potential models, see Eqs. (34), (35), (36), and Appendix C.

The most attractive feature of the boost-invariant Hamiltonian approach to heavy quarkonia, the one that makes it an interesting candidate for a new expansion method in solving QCD [3], is that the renormalization group procedure for effective particles can be systematically studied order by order in expansion in powers of the effective coupling constant α_λ with λ on the order of quark masses. Such expansion may provide a reasonably converging sequence of approximations if α_λ is much smaller than 1. This study shows that $\alpha \sim 1/3$ is a reasonable candidate to reproduce the masses of $b\bar{b}$ and $c\bar{c}$ mesons in systematic calculations. Genuine 4th-order RGPEP studies will further clarify if this hope is

realistic.

On the other hand, careful readers have certainly observed that the LF Hamiltonian dynamics with a harmonic oscillator potential leads to the eigenvalues M^2 that are proportional to the angular momentum in the relative motion of quarks, like in Regge trajectories. This is a phenomenologically desired feature, although one cannot trust the oscillator picture over large distances. But when one considers highly excited states, their masses increasing as dictated by the quadratic potential, the probability of emission of effective gluons will be also increasing. A string of gluons may be formed, with new potentials between heavy effective gluons that require further investigation. The Hamiltonian approach could thus lead to a quantum theory of the gluon string and provide another reason for the same Regge-like behavior of the spectrum, with a different slope than implied by the two-quark approximation and with validity extending to much larger distances than the size of a typical hadron. In fact, for a firm chain of quantum gluons to form a string, each pair of the neighboring gluons must be held together stronger than by a linear potential, and a quadratic potential satisfies this condition. The pilot calculation described here suggests that the oscillator frequencies are on the order of one inverse fermi, and the oscillator potential term grows as the relative distance squared in fermis with a coefficient given by the quark mass. This means that the oscillator potential is strong for the inter-quark distances larger than about a fermi and the quantum theory of the gluon strings with a similar potential between gluons may turn out to be useful in phenomenology. Thus, the structure emerging in this pilot study of the boost-invariant Hamiltonian approach to QCD has a reasonable chance to grow toward a realistic physical picture supported by a mathematically well-defined theory. This is more than another reason to undertake the 4th-order studies of the approach.

Acknowledgement

This work was supported in part by the Grants No. KBN 1 P03B 117 26 and MNiSW BST-975/BW-1640.

APPENDIX A: TERMS IN H_λ

This appendix lists details of terms in Eq. (20) for H_λ . The kinetic energy term for effective quarks reads

$$T_{q\lambda} = \sum_{\sigma c} \int [k] \frac{k^\perp 2 + m_\lambda^2}{k^+} \left[b_{\lambda k \sigma c}^\dagger b_{\lambda k \sigma c} + d_{\lambda k \sigma c}^\dagger d_{\lambda k \sigma c} \right], \quad (A1)$$

and for certain $\lambda = \lambda_0$ one can set

$$\begin{aligned} m_{\lambda_0}^2 &= m^2 + \frac{4}{3} g^2 \int [x\kappa] \tilde{r}_\delta^2(x) f_{\lambda_0}^2(m^2, \mathcal{M}^2) \\ &\times \frac{j^{\mu*} j^\nu \left[-g_{\mu\nu} + \frac{n_\mu n_\nu}{p^+ 2} \frac{\mathcal{M}^2 - m^2}{x} \right]}{\mathcal{M}^2 - m^2}, \end{aligned} \quad (A2)$$

with $\mathcal{M}^2 = \kappa^{\perp 2}/x + (\kappa^{\perp 2} + m^2)/(1-x)$. The integration measure $[x\kappa]$ stands for $dx d^2\kappa^{\perp}/[16\pi^3 x(1-x)]$. That the effective mass does not depend on the particle motion is a unique property of the RGPEP in LF dynamics. $\tilde{r}_{\delta}(x)$ denotes the small- x regularization factors $r_{\delta}(x)r_{\delta}(1-x)$, where $r_{\delta}(x) = x^{\delta}\theta(x)$. The gluon kinetic energy term reads,

$$T_{g\lambda} = \sum_{\sigma c} \int [k] \frac{k^{\perp 2} + \mu_{\lambda}^2}{k^+} a_{\lambda k \sigma c}^{\dagger} a_{\lambda k \sigma c}, \quad (\text{A3})$$

but an explicit expression for μ_{λ}^2 [34, 35] is not needed in this work.

The emission and absorption term, $Y_{\lambda} = f_{\lambda} Y_{qg\lambda}$, is

$$Y_{\lambda} = g \sum_{123} \int [123] r_{\delta}(x_{1/3}) r_{\delta}(x_{2/3}) f_{\lambda}(\mathcal{M}_{12}^2, m^2) \times \left[j_{23} b_{\lambda 2}^{\dagger} a_{\lambda 1}^{\dagger} b_{\lambda 3} + \bar{j}_{23} d_{\lambda 2}^{\dagger} a_{\lambda 1}^{\dagger} d_{\lambda 3} + h.c. \right], \quad (\text{A4})$$

where $j_{23} = \tilde{\delta} t_{23}^1 g_{\mu\nu} j_{23}^{\mu} \varepsilon_1^{\nu*}$, $\bar{j}_{23} = \tilde{\delta} t_{32}^1 g_{\mu\nu} \bar{j}_{32}^{\mu} \varepsilon_1^{\nu*}$, $\tilde{\delta}$ denotes the δ -function of three-momentum conservation times $16\pi^3$, t^a with $a = 1, \dots, 8$ denote 3×3 matrices of generators of color $SU(3)$ gauge transformations for quarks, ε is the gluon polarization four-vector, $j_{23}^{\mu} = \bar{u}_2 \gamma^{\mu} u_3$ and $\bar{j}_{32}^{\mu} = \bar{v}_3 \gamma^{\mu} v_2$.

The potential term, $V_{\lambda} = f_{\lambda} V_{q\bar{q}\lambda}$, is

$$V_{\lambda} = -g^2 \sum_{1234} \int [1234] \tilde{\delta} t_{12}^a t_{43}^a V_{\lambda}(13, 24) b_1^{\dagger} d_3^{\dagger} d_4 b_2, \quad (\text{A5})$$

where (see Ref. [4])

$$V_{\lambda}(13, 24) = \frac{d_{\mu\nu}(k_5)}{k_5^+} j_{12}^{\mu} \bar{j}_{43}^{\nu} f_{\lambda}(\mathcal{M}_{13}^2, \mathcal{M}_{24}^2) \times \left[\theta(z) \tilde{r}_{\delta}(x_{5/1}) \tilde{r}_{\delta}(x_{5/4}) \mathcal{F}_{2\lambda}(1, 253, 4) + \theta(-z) \tilde{r}_{\delta}(x_{5/3}) \tilde{r}_{\delta}(x_{5/2}) \mathcal{F}_{2\lambda}(3, 154, 2) \right], \quad (\text{A6})$$

and, for example,

$$\frac{\mathcal{F}_{2\lambda}(1, 253, 4)}{P^+} = \frac{x_1(\mathcal{M}_{52}^2 - m^2) + x_4(\mathcal{M}_{53}^2 - m^2)}{(\mathcal{M}_{52}^2 - m^2)^2 + (\mathcal{M}_{53}^2 - m^2)^2} \times \left[\exp \left[-\frac{(\mathcal{M}_{52}^2 - m^2)^2 + (\mathcal{M}_{53}^2 - m^2)^2}{\lambda^4} \right] - 1 \right]. \quad (\text{A7})$$

$\mathcal{M}_{ij} = (k_i + k_j)^2$ is the invariant mass of particles i and j . Momenta are labeled according to Fig. 7. P^+ denotes the sum of plus momenta of annihilated quarks. The sum

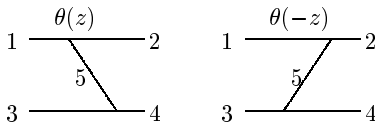


FIG. 7: Momentum labels in potential terms.

over gluon polarizations,

$$d_{\mu\nu}(k_5) = -g_{\mu\nu} + \frac{n^{\mu} k_5^{\nu} + k_5^{\mu} n^{\nu}}{k_5^+}, \quad (\text{A8})$$

involves momentum $k_5^{+, \perp} = \varepsilon(z)(k_1^{+, \perp} - k_2^{+, \perp})$ with $\varepsilon(z) = \theta(z) - \theta(-z)$, and $z = (k_1^+ - k_2^+)/(k_1^+ + k_2^+)$. $x_5 = |z|$, and $k_5^- = k_5^{+2}/k_5^+$. The instantaneous interaction between effective quarks, $Z_{\lambda} = f_{\lambda} Z_{q\bar{q}\lambda}$, is

$$Z_{\lambda} = -g^2 \sum_{1234} \int [1234] \tilde{\delta} t_{12}^a t_{43}^a Z_{\lambda}(13, 24) b_{\lambda 1}^{\dagger} d_{\lambda 3}^{\dagger} d_{\lambda 4} b_{\lambda 2}, \quad (\text{A9})$$

where

$$Z_{\lambda}(13, 24) = \frac{1}{k_5^{+2}} j_{12}^+ \bar{j}_{34}^+ f_{\lambda}(\mathcal{M}_{13}^2, \mathcal{M}_{24}^2) \times \left[\theta(z) \tilde{r}_{\delta}(x_{5/1}) \tilde{r}_{\delta}(x_{5/4}) + \theta(-z) \tilde{r}_{\delta}(x_{5/3}) \tilde{r}_{\delta}(x_{5/2}) \right]. \quad (\text{A10})$$

APPENDIX B: RGPEP SCALING WITH α

This appendix includes contributions that originate in the $g_{\mu\nu}$ -parts of the sums over gluon polarizations, which were not explicitly described in Ref. [4].

The analysis of scaling with α_0 for RGPEP factors in the window eigenvalue equation for H_{λ_0} with a mass ansatz μ^2 is based on the similarity between the structure of the eigenvalue Eq. (39) and the Schrödinger equation with Coulomb potential in QED (the same kind of the leading picture is also found in Yukawa theory [42]). The subscripts λ_0 and 0 are often omitted to simplify notation.

When the relative momentum of electron and positron in positronium is written as

$$\vec{k} = \alpha \mu \vec{p}, \quad (\text{B1})$$

where μ is the reduced mass of the fermions, the Schrödinger equation for positronium, neglecting spin effects,

$$\frac{k^2}{2\mu} \psi(\vec{k}) - \int \frac{d^3 k'}{(2\pi)^3} \frac{4\pi\alpha}{(\vec{k} - \vec{k}')^2} \psi(\vec{k}') = E \psi(\vec{k}), \quad (\text{B2})$$

takes the form

$$p^2 \phi(\vec{p}) - 2 \int \frac{d^3 p'}{(2\pi)^3} \frac{4\pi}{(\vec{p} - \vec{p}')^2} \phi(\vec{p}') = x \phi(\vec{p}). \quad (\text{B3})$$

The eigenvalue is $E = x \frac{1}{2} \mu \alpha^2$, and the ground-state has the eigenvalue $E = E_0$ with $x = x_0 = -1$ and wave function

$$\phi_0(\vec{p}) = \frac{N_p}{(p^2 + 1)^2}. \quad (\text{B4})$$

Higher states have $x = -1/n^2$ with natural n greater than 1.

In the QCD Schrödinger equation with $H_{Q\bar{Q}\lambda}$, the self-interaction terms and the potential kernel contain similar expressions. The self-interaction terms are easy to

analyze if one knows how to analyze the structure of v_λ in the eigenvalue Eq. (39). At certain $\lambda = \lambda_0$, with λ_0 parameterized according to Eq. (42), one has $v_{\lambda_0}(13, 24) = v_0(13, 24)$ and

$$v_0 = -A g_{\mu\nu} j_{12}^\mu \bar{j}_{43}^\nu + B \frac{j_{12}^+ \bar{j}_{43}^+}{P^+}, \quad (\text{B5})$$

$$A = \frac{1}{|z|} \left[f_0(13, 24) \frac{V}{P^+} + \frac{1}{2} w_0(13, 24) \right], \quad (\text{B6})$$

$$B = \frac{1}{z^2} \frac{d}{|z|} \left[f_0(13, 24) \frac{V}{P^+} + \frac{1}{2} w_0(13, 24) \right] + \frac{1}{z^2} f_0(13, 24) Z, \quad (\text{B7})$$

where

$$V = \theta(z) \tilde{r}_\delta(x_{5/1}) \tilde{r}_\delta(x_{5/4}) \mathcal{F}_{2\lambda}(1, 253, 4) + \theta(-z) \tilde{r}_\delta(x_{5/3}) \tilde{r}_\delta(x_{5/2}) \mathcal{F}_{2\lambda}(3, 154, 2), \quad (\text{B8})$$

$$Z = \theta(z) \tilde{r}_\delta(x_{5/1}) \tilde{r}_\delta(x_{5/4}) + \theta(-z) \tilde{r}_\delta(x_{5/3}) \tilde{r}_\delta(x_{5/2}), \quad (\text{B9})$$

$$\begin{aligned} \frac{w_0}{|z|} = & \frac{\theta(z) \tilde{r}_\delta(x_{5/1}) \tilde{r}_\delta(x_{5/4}) f_{52} f_{53}}{|z|(m^2 - \mathcal{M}_{52}^2)/x_1 - \mu^2(2, 5, 3)} \\ & + \frac{\theta(-z) \tilde{r}_\delta(x_{5/3}) \tilde{r}_\delta(x_{5/2}) f_{54} f_{51}}{|z|(m^2 - \mathcal{M}_{54}^2)/x_3 - \mu^2(1, 5, 4)} \\ & + \frac{\theta(z) \tilde{r}_\delta(x_{5/1}) \tilde{r}_\delta(x_{5/4}) f_{52} f_{53}}{|z|(m^2 - \mathcal{M}_{53}^2)/x_4 - \mu^2(2, 5, 3)} \\ & + \frac{\theta(-z) \tilde{r}_\delta(x_{5/3}) \tilde{r}_\delta(x_{5/2}) f_{54} f_{51}}{|z|(m^2 - \mathcal{M}_{51}^2)/x_2 - \mu^2(1, 5, 4)}, \end{aligned} \quad (\text{B10})$$

$$\begin{aligned} \frac{d}{|z|} = & \theta(z) \left(\frac{\mathcal{M}_{52}^2 - m^2}{2x_1} + \frac{\mathcal{M}_{53}^2 - m^2}{2x_4} \right) \\ & + \theta(-z) \left(\frac{\mathcal{M}_{51}^2 - m^2}{2x_2} + \frac{\mathcal{M}_{54}^2 - m^2}{2x_3} \right), \end{aligned} \quad (\text{B11})$$

and f_{ij} denotes $f_{\lambda_0}[m^2, (k_i + k_j)^2]$.

In order to describe the structure of v_0 for relative quark momenta comparable with the strong Bohr momentum, introduced in Eq. (41), it is convenient to write expressions for $\mathcal{F}(1, 253, 4)/k_5^+$ and $\mathcal{F}(3, 154, 2)/k_5^+$ that contribute to V using identities

$$\mathcal{M}_{253}^2 = \frac{\mathcal{M}_{52}^2 - m^2}{x_1} + \mathcal{M}_{13}^2 = \frac{\mathcal{M}_{53}^2 - m^2}{x_4} + \mathcal{M}_{24}^2, \quad (\text{B12})$$

$$\mathcal{M}_{154}^2 = \frac{\mathcal{M}_{54}^2 - m^2}{x_3} + \mathcal{M}_{13}^2 = \frac{\mathcal{M}_{51}^2 - m^2}{x_2} + \mathcal{M}_{24}^2. \quad (\text{B13})$$

One starts with expressions, see Eq. (A7),

$$\begin{aligned} \frac{\mathcal{F}_2(1, 253, 4)}{k_5^+} = & \frac{1}{|z|} \frac{x_1 (\mathcal{M}_{52}^2 - m^2) + x_4 (\mathcal{M}_{53}^2 - m^2)}{(\mathcal{M}_{52}^2 - m^2)^2 + (\mathcal{M}_{53}^2 - m^2)^2} \\ & \times (ff - 1), \end{aligned} \quad (\text{B14})$$

$$\begin{aligned} \frac{\mathcal{F}_2(3, 154, 2)}{k_5^+} = & \frac{1}{|z|} \frac{x_2 (\mathcal{M}_{51}^2 - m^2) + x_3 (\mathcal{M}_{54}^2 - m^2)}{(\mathcal{M}_{51}^2 - m^2)^2 + (\mathcal{M}_{54}^2 - m^2)^2} \\ & \times (ff - 1), \end{aligned} \quad (\text{B15})$$

where

$$\mathcal{M}_{51}^2 - m^2 = \mathcal{D}_1, \quad (\text{B16})$$

$$\mathcal{M}_{52}^2 - m^2 = \frac{x_1}{x_2} \mathcal{D}_1, \quad (\text{B17})$$

$$\mathcal{M}_{53}^2 - m^2 = \mathcal{D}_3, \quad (\text{B18})$$

$$\mathcal{M}_{54}^2 - m^2 = \frac{x_3}{x_4} \mathcal{D}_3, \quad (\text{B19})$$

and

$$\mathcal{D}_1 = \frac{x_1}{|z|} \left[\left(q^\perp - \frac{z}{x_1} k_{13}^\perp \right)^2 + m^2 \frac{z^2}{x_1^2} \right], \quad (\text{B20})$$

$$\mathcal{D}_3 = \frac{x_3}{|z|} \left[\left(q^\perp + \frac{z}{x_3} k_{13}^\perp \right)^2 + m^2 \frac{z^2}{x_3^2} \right]. \quad (\text{B21})$$

The definitions include

$$z = x_1 - x_2, \quad (\text{B22})$$

and it is helpful to use three-dimensional CMF relative momentum variables \vec{k}_{13} and \vec{k}_{24} , and $\vec{q} = \vec{k}_{13} - \vec{k}_{24}$. So, for $ij = 13$ and 24 ,

$$x_i = \frac{1}{2} + \frac{k_{ij}^3}{2\sqrt{m^2 + \vec{k}_{ij}^2}}, \quad (\text{B23})$$

and

$$z = \frac{k_{13}^3}{\mathcal{M}_{13}} - \frac{k_{24}^3}{\mathcal{M}_{24}}. \quad (\text{B24})$$

The first step is to establish that the potential does not generate any small- x singularities in its fully relativistic form [4]. The next step is to analyze scaling with α . The key to scaling with α for given quark mass m is the substitution

$$\vec{k}_{ij} = k_B \vec{p}_{ij}, \quad (\text{B25})$$

where k_B is the strong Bohr momentum of Eq. (41). The dimensionless variables \vec{p}_{ij} , with $ij = 13$ or 24 , are typically on the order of 1 in both the purely Coulombic case of QED and in the QCD case that includes the harmonic oscillator potential studied here. A dimensionless momentum transfer \vec{p} is defined by

$$\vec{q} = k_B \vec{p}, \quad (\text{B26})$$

so that $\vec{p} = \vec{p}_{13} - \vec{p}_{24}$. Factors ff limit $|\vec{p}|$ to values order $(4\alpha/3)^{2\epsilon} \lambda_p^2$, and the additional damping due to $\epsilon > 0$ provides a possibility to formally separate the dominant terms in the limit $\alpha \rightarrow 0$ because the Coulomb eigenvalue problem is dominated by the dimensionless momenta p_{ij} on the order of 1. The outer-most factor f_0 in the potential terms limits changes of momenta p_{ij} from above by $\alpha^{\epsilon-0.5}$ and this f_0 becomes irrelevant for very small α , leaving the Coulomb interaction and the harmonic oscillator term that provide the leading approximation.

Observe that

$$\frac{\mathcal{F}_2(1, 253, 4)}{k_5^+(ff-1)} = \frac{(\mathcal{M}_{253}^2 - C_{253})|z|^{-1}}{\mathcal{M}_{253}^4 - 2\mathcal{M}_{253}^2C_{253} + D_{253}}, \quad (\text{B27})$$

$$\frac{\mathcal{F}_2(3, 154, 2)}{k_5^+(ff-1)} = \frac{(\mathcal{M}_{154}^2 - C_{154})|z|^{-1}}{\mathcal{M}_{154}^4 - 2\mathcal{M}_{154}^2C_{154} + D_{154}}, \quad (\text{B28})$$

where

$$C_{253} = \frac{x_1^2\mathcal{M}_{13}^2 + x_4^2\mathcal{M}_{24}^2}{x_1^2 + x_4^2}, \quad (\text{B29})$$

$$D_{253} = \frac{x_1^2\mathcal{M}_{13}^4 + x_4^2\mathcal{M}_{24}^4}{x_1^2 + x_4^2}, \quad (\text{B30})$$

$$C_{154} = \frac{x_3^2\mathcal{M}_{13}^2 + x_2^2\mathcal{M}_{24}^2}{x_3^2 + x_2^2}, \quad (\text{B31})$$

$$D_{154} = \frac{x_3^2\mathcal{M}_{13}^4 + x_2^2\mathcal{M}_{24}^4}{x_3^2 + x_2^2}. \quad (\text{B32})$$

Using Eq. (B25), and introducing two three-vectors,

$$\vec{\xi} = \frac{\vec{k}_{13} + \vec{k}_{24}}{m} = O(\alpha), \quad (\text{B33})$$

$$\vec{t} = \vec{q}/q, \quad (\text{B34})$$

one obtains

$$\mathcal{M}_{253}^2 - C_{253} = \mathcal{M}_{154}^2 - C_{154} + \frac{O(\alpha^5)}{|z|} \quad (\text{B35})$$

$$= \frac{q^2}{|z|} \left(1 - \iota_z \xi_z \vec{t} \vec{\xi} \right) + \frac{O(\alpha^5)}{|z|}, \quad (\text{B36})$$

$$D_{253} - C_{253}^2 = D_{154} - C_{154}^2 + \frac{O(\alpha^7)}{z^2} \quad (\text{B37})$$

$$= \frac{q^4}{z^2} \iota_z^2 \left(\vec{t} \vec{\xi} \right)^2 + \frac{O(\alpha^7)}{z^2}. \quad (\text{B38})$$

Thus,

$$\frac{\mathcal{F}_2(1, 253, 4)}{k_5^+(ff-1)} = \frac{\mathcal{F}_2(3, 154, 2)}{k_5^+(ff-1)} + O(\alpha) \quad (\text{B39})$$

$$= \frac{1}{q^2} + \frac{\iota_z \xi_z \vec{t} \vec{\xi} - \iota_z^2 (\vec{t} \vec{\xi})^2}{q^2} + O(\alpha). \quad (\text{B40})$$

The effective-gluon exchange term w_0 in Eq. (B10), is

$$\frac{w_0}{|z|} = -\frac{2\theta(z)\tilde{r}_\delta(x_{5/1})\tilde{r}_\delta(x_{5/4})f_{52}f_{53}}{q^2 + \mu^2(2, 5, 3) + O(\alpha^{3+4\epsilon})} - \frac{2\theta(-z)\tilde{r}_\delta(x_{5/3})\tilde{r}_\delta(x_{5/2})f_{54}f_{51}}{q^2 + \mu^2(1, 5, 4) + O(\alpha^{3+4\epsilon})}, \quad (\text{B41})$$

and the intermediate gluon spin sum contributes

$$d = q^2 + O(\alpha^6). \quad (\text{B42})$$

In summary, the factors A and B , defined in Eqs. (B6) and (B7), scale as

$$A \simeq -f_0 \frac{1}{q^2} \left[1 - \frac{ff}{f_0} \left(f_0 - \frac{q^2}{q^2 + \mu^2} \right) + c \right], \quad (\text{B43})$$

$$B \simeq -f_0 \frac{4m^2}{q_z^2} \left[-\frac{ff}{f_0} \left(f_0 - \frac{q^2}{q^2 + \mu^2} \right) + c \right], \quad (\text{B44})$$

$$c = \vec{e}_z \vec{t} \vec{\xi} \left(\vec{e}_z \vec{\xi} - \vec{e}_z \vec{t} \vec{\xi} \right) + O(\alpha^3), \quad (\text{B45})$$

and $c \sim \alpha^2$ because $|\vec{\xi}| = O(\alpha)$. These scaling results are valid even if the mass ansatz μ^2 is of the order of α instead of 1.

Scaling analysis of the self-interaction terms begins with the RGPEP expression for renormalized effective quark mass terms in the eigenvalue Eq. (39),

$$\begin{aligned} \frac{\delta m_i^2}{x_i} &= \frac{4g^2}{3x_i} \int [y\rho] f^2(m^2, \mathcal{M}^2) \frac{2}{1-y} \\ &\times \left\{ m^2 y^2 + [1 + (1-y)^2] \left(\frac{\rho^\perp}{y} \right)^2 \right\} \\ &\times \left[\frac{1}{\mathcal{M}^2 - m^2} - \frac{1}{\mathcal{M}_i^2 - m^2} \right]. \end{aligned} \quad (\text{B46})$$

where

$$\mathcal{M}_i^2 - m^2 = \mathcal{M}^2 - m^2 + \frac{\mu^2}{y}, \quad (\text{B47})$$

$$\mathcal{M}^2 - m^2 = \frac{\rho^\perp 2 + y^2 m^2}{y(1-y)}, \quad (\text{B48})$$

and μ^2 is the mass ansatz for the effective gluon accompanying the quarks i' and j . One can introduce the variable

$$q^\perp = \rho^\perp, \quad q_z = ym, \quad (\text{B49})$$

and observe that when $\lambda_0 \sim \alpha^{0.5+\epsilon}m$, the magnitude of q is limited by the RGPEP form factor f^2 to the range between 0 and $\alpha^{1+2\epsilon}m$. Corrections order y cancel out or multiply terms order q^2 . If μ^2 is of order 1, deviations from $y = 0$ introduce corrections order $\alpha^{4+6\epsilon}$ and can be formally neglected when one keeps only terms order α^2 and α^4 . Note that the terms order α^3 cancel out completely, and even for μ^2 order α the first correction due to $y \neq 1$ is order $\alpha^{4+6\epsilon}$. Then, since the integrand is symmetric in $t = \cos \theta$, where $q_z = qt$, and since $x_1 x_2$ differs from 1/4 in order α^2 , the leading contribution from the self-interactions is

$$\begin{aligned} \frac{\delta m_1^2}{x_1} + \frac{\delta m_3^2}{x_3} &= 8m \frac{4}{3} \frac{g^2}{16\pi^3} \int d^3q \\ &\times ff \left(\frac{1}{q_z^2} - \frac{1}{q^2} \right) \frac{\mu^2}{\mu^2 + q^2}. \end{aligned} \quad (\text{B50})$$

APPENDIX C: SPINORS

The 4×4 matrix wave function Ψ_{ij} in Eq. (35), is written using spinors $u_{k,s}$ and $v_{k,s}$ that are obtained by applying matrix $B(k, m)$ from Eq. (37) to spinors at rest, $u_{0,s}$ and $v_{0,s}$, which are defined as

$$u_{0,s} = \sqrt{2m} \begin{bmatrix} \chi_s \\ 0 \end{bmatrix}, \quad (\text{C1})$$

$$v_{0,s} = 2s\sqrt{2m} \begin{bmatrix} 0 \\ \chi_{\bar{s}} \end{bmatrix}. \quad (\text{C2})$$

χ_s denotes standard two-component spinors, with upper component equal $1/2 + s$ and lower $1/2 - s$, and \bar{s} means $-s$. Instead of $s = \pm 1/2$, $\sigma = 2s$ with values ± 1 is often used below. The above spinors correspond to fermions at rest in the frame of reference in which one carries out the calculation for the bound state with momentum components P^+ and P^\perp . The discussion below is simplified to the case $P^\perp = 0$ since the transverse motion of the bound state does not introduce any change in the final formulas.

The wave function $\Psi(\vec{k}_{ij}, s_i, s_j)$ in Eq. (36) is defined using the matrix $\Psi_{CMFij}(\vec{k}_{ij})$ and spinors $u_{\vec{k}_{ij}, s_i}$ and $v_{-\vec{k}_{ij}, s_j}$ that describe the fermions in the CMF of the quarks i and j . These are obtained by standard matrices for boosts along \vec{k}_{ij} instead of the LF boosts. Namely,

$$u_{\vec{k}, \sigma} = L(\vec{k}) \sqrt{2m} \begin{bmatrix} \tilde{\chi}_{\vec{k}, \sigma} \\ 0 \end{bmatrix}, \quad (C3)$$

$$v_{\vec{k}, \sigma} = L(\vec{k}) \sigma \sqrt{2m} \begin{bmatrix} 0 \\ \tilde{\chi}_{\vec{k}, \sigma} \end{bmatrix}, \quad (C4)$$

$$L(\vec{k}) = \frac{1}{\sqrt{2m(E_k + m)}} [\vec{k} + \beta m] \beta. \quad (C5)$$

The two component spinors at rest are turned away from the z -axis using a 2×2 matrix $\zeta(\vec{k})$:

$$\tilde{\chi}_{\vec{k}, \sigma} = \zeta(\vec{k}) \chi_\sigma, \quad (C6)$$

$$\zeta(\vec{k}) = \sqrt{\frac{k^+}{m}} \frac{\sqrt{2m(E_k + m)}}{(k^+ + m)^2 + k^\perp{}^2} (k^+ + m + \sigma^\perp k^\perp \sigma^3). \quad (C7)$$

The matrix ζ introduces the spinor basis in which the wave function $\Psi_{CMFij}(\vec{k}_{ij})$ satisfies a rotationally symmetric eigenvalue equation in the leading approximation. The matrix ζ has been used before by Melosh [44] as a candidate for description of how the constituent quarks are related to current quarks, and by Brisudova and Perry [45] in LF eigenvalue problems. Here, the constituent quarks are dynamically related to current quarks using RGPEP and ζ plays only the kinematical role of choosing a basis for spinors. The matrix ζ is needed because there is a change of frame of reference involved in expressing LF spinors in the frame of reference in which the whole quarkonium has momentum P^+ and $P^\perp = 0$ in terms of the spinors in the CMF of the pair of quarks. For example, $u_{k_1, s_1} = \mathcal{L}_{13} u_{\vec{k}_{13}, s_1}$, where

$$\mathcal{L}_{ij} = \Lambda^+ \sqrt{\frac{P^+}{\mathcal{M}_{ij}}} + \Lambda^- \sqrt{\frac{\mathcal{M}_{ij}}{P^+}}. \quad (C8)$$

When one uses the slightly rotated basis for the two-component spinors in the CMF of fermions, as indicated in Eqs. (C3) and (C4), and then calculates the spinors in the frame of reference where the bound state eigenvalue P^- is calculated, one obtains spinors that are used in Eq.

(34). E.g.,

$$u_i = \mathcal{L}_{ij} B(k_{ij}, m) \zeta^{-1}(\vec{k}_{ij}) L^{-1}(\vec{k}_{ij}) u_{\vec{k}_{13}, s_1}. \quad (C9)$$

The matrix ζ is defined to render

$$B(k_{13}, m) \zeta^{-1}(\vec{k}_{13}) L^{-1}(\vec{k}_{13}) = 1, \quad (C10)$$

and $u_1 = \mathcal{L}_{13} u_{\vec{k}_{13}, s_1}$. Similarly, $u_2 = \mathcal{L}_{24} u_{\vec{k}_{24}, s_2}$, $v_3 = \mathcal{L}_{13} v_{-\vec{k}_{13}, s_3}$, and $v_4 = \mathcal{L}_{24} v_{-\vec{k}_{24}, s_4}$.

APPENDIX D: BREIT-FERMI TERMS

In the leading approximation for small α , the potential kernel given in Eq. (40) is

$$v_0 = f \frac{1}{q^2} g_{\mu\nu} j_{12}^\mu \bar{j}_{43}^\nu + ff \frac{\mu^2}{q^2 + \mu^2} \left[\frac{4m^2 j_{12}^+ \bar{j}_{43}^+}{P^+{}^2 q_z^2} - \frac{g_{\mu\nu} j_{12}^\mu \bar{j}_{43}^\nu}{q^2} \right]. \quad (D1)$$

The Breit-Fermi terms in this article originate from the first term. Note that the first term contains only one form factor and this form factor limits the change of the square of the dimensionless momentum p_{ij} in the scaling analysis by a number of the order of $\alpha^{2\epsilon-1}$, which is much larger than 1 when $0 < \epsilon < \frac{1}{2}$, see Appendix B. In contrast, the second term contains two form factors and in the scaling analysis these form factors limit the dimensionless momentum transfer $p = |\vec{p}|$ between quarks by a small number on the order of $(|p_z|/p)\lambda_p^2(4\alpha/3)^{2\epsilon}$, see Section III D and Appendix B. This difference between the form factors implies, that in the first term the dominant momentum scale is of order 1, originating from the Coulomb potential, while in the second term the allowed momentum exchange p is in principle infinitesimal as long as $\epsilon > 0$. Thus, the second term would be negligible in the scaling analysis if it did not contain the diverging factor q_z^{-2} . This divergence is regulated by the falloff of the ansatz μ^2 as a function of q_z when q_z tends to zero, as required by the condition that the ansatz does not produce a small- x divergence [4].

In the leading approximation, the current factors are diagonal in spin: $j_{12}^\mu \bar{j}_{43\mu}$ equals $4m^2$, and $j_{12}^+ \bar{j}_{43}^+$ always equals $4P^+{}^2$ times $\sqrt{x_1 x_2 x_3 x_4}$. The square root reduces to $1/4$ since all the x s differ from $1/2$ only by terms of order α or smaller. In this case, the second term in Eq. (D1) is the same as the integrand in Eq. (B50) for self-interactions. The self-interaction and the second term in Eq. (D1) produce together [4] the harmonic oscillator potential in Eq. (50) with the dimensionless spring constant given in Eq. (53).

Beyond the leading order, one has to analyze the factor $j_{12}^\mu \bar{j}_{43\mu}$. It can be re-written in a matrix notation of Eq. (51). The *BF* terms in the potential kernel \mathcal{V} act on the 2×2 matrix wave function ϕ which is defined as follows.

Using results from Appendix C, the sum over quark spins in Eq. (39) can be written as

$$\sum_{s_2 s_4} j_{12}^\mu \bar{j}_{43\mu} \Psi_{s_2 s_4}(\vec{k}_{24}) = \quad (D2)$$

$$\bar{u}_{\vec{k}_{13}, s_1} \gamma^0 \mathcal{L}_{13}^\dagger \gamma^0 \gamma^\mu \mathcal{L}_{24} K_{24} \gamma^0 \mathcal{L}_{24}^\dagger \gamma^0 \gamma_\mu \mathcal{L}_{13} v_{-\vec{k}_{13}, s_3},$$

$$K_{ij} = (\not{k}_{ij} + m) \Psi_{CMFij}(\vec{k}_{ij}) (\not{k}_{ij} - m), \quad (D3)$$

where $k = (k^0, \vec{k})$, $\bar{k} = (k^0, -\vec{k})$, and $k^0 = \sqrt{m^2 + \vec{k}^2}$. This 4×4 matrix notation can be replaced by a 2×2 matrix notation using

$$\Psi_{s_i s_j}(\vec{k}_{ij}) = \bar{u}_{\vec{k}_{ij}, s_i} \Psi_{CMFij}(\vec{k}_{ij}) v_{-\vec{k}_{ij}, s_j}$$

$$\equiv \sqrt[4]{1 + \vec{k}_{ij}^2/m^2} \sigma_j \tilde{\chi}_i^\dagger \phi(\vec{p}_{ij}) \tilde{\chi}_j, \quad (D4)$$

where

$$\phi(\vec{p}_{ij}) = a + \vec{b} \cdot \vec{\sigma} \quad (D5)$$

is the wave function that appears in Eq. (50): a and \vec{b} are together four functions of the dimensionless relative momentum \vec{p}_{ij} . The fourth root in front of ϕ is introduced because the measure factor,

$$\int \frac{dx_2 d^2 \kappa_{24}^\perp}{x_2 x_4} = \int \frac{2d^3 k_{24}}{\sqrt{m^2 + k_{24}^2}}, \quad (D6)$$

needs to be symmetrized with respect to relative momenta \vec{k}_{24} and \vec{k}_{13} . The resulting potential contains a product of $\sqrt[4]{1 + \vec{k}_{13}^2/m^2}$ and $\sqrt[4]{1 + \vec{k}_{24}^2/m^2}$ in denominator, and the integration measure becomes $d^3 k_{24}$ like in a non-relativistic Schrödinger equation. Thus, the leading contribution of the measure to BF terms through M in Eqs. (49) and (51) is

$$M = -\frac{1}{16} \left(\frac{4}{3} \alpha \right)^2 (\vec{p}_{13}^2 + \vec{p}_{24}^2). \quad (D7)$$

The spin contribution $1 + \alpha^2 S$ in Eq. (49) is obtained from the sum over quark spins

$$\sum_{s_2 s_4} \frac{j_{12}^\mu \bar{j}_{43\mu}}{4m^2} \frac{\Psi_{s_2 s_4}(\vec{k}_{24})}{\sqrt[4]{1 + \vec{k}_{24}^2/m^2}}, \quad (D8)$$

using the two component spinors in Eq. (C6) and the wave function in Eq. (D5). One multiplies the whole eigenvalue equation by $\tilde{\chi}_1$ from the left and by $\sigma_3 \tilde{\chi}_3$ from the right and sums up over spins 1 and 3. Then, the kinetic energy multiplies only the matrix $\phi(\vec{p}_{13})$, and the potential term contains the matrix

$$\frac{S_l^\mu \phi(\vec{p}_{24}) S_{r\mu}}{4m^2(E_{k_{13}} + m)(E_{k_{24}} + m)}, \quad (D9)$$

where, using $\alpha^\mu = \gamma^0 \gamma^\mu$ and notation from Ref. [65],

$$S_l^\mu = [E_{13} + m, \vec{k}_{13} \vec{\sigma}] \mathcal{L}_{13} \alpha^\mu \mathcal{L}_{24} \left[\begin{smallmatrix} E_{24} + m \\ \vec{k}_{24} \vec{\sigma} \end{smallmatrix} \right], \quad (D10)$$

$$S_r^\mu = [-\vec{k}_{24} \vec{\sigma}, E_{24} + m] \mathcal{L}_{24} \alpha^\mu \mathcal{L}_{13} \left[\begin{smallmatrix} -\vec{k}_{13} \vec{\sigma} \\ E_{13} + m \end{smallmatrix} \right]. \quad (D11)$$

When one neglects terms that vanish faster than α^2 in the scaling analysis, the matrices \mathcal{L}_{13} and \mathcal{L}_{24} are equivalent to 1 and the resulting matrix in the potential takes a fully rotationally symmetric form,

$$\frac{[E_{13} + m, \vec{k}_{13} \vec{\sigma}] \alpha^\mu \left[\begin{smallmatrix} E_{24} + m \\ \vec{k}_{24} \vec{\sigma} \end{smallmatrix} \right] \phi [-\vec{k}_{24} \vec{\sigma}, E_{24} + m] \alpha_\mu \left[\begin{smallmatrix} -\vec{k}_{13} \vec{\sigma} \\ E_{13} + m \end{smallmatrix} \right]}{4m^2(E_{k_{13}} + m)(E_{k_{24}} + m)}. \quad (D12)$$

The result is $\phi + (4\alpha/3)^2 S/16$, where

$$S = (p_{13}^2 + p_{24}^2) \phi + \vec{p}_{13} \vec{\sigma} \vec{p}_{24} \vec{\sigma} \phi + \phi \vec{p}_{24} \vec{\sigma} \vec{p}_{13} \vec{\sigma}$$

$$+ \sigma^i \vec{p}_{24} \vec{\sigma} \phi \vec{p}_{24} \vec{\sigma} \sigma^i + \sigma^i \vec{p}_{24} \vec{\sigma} \phi \sigma^i \vec{p}_{13} \vec{\sigma}$$

$$+ \vec{p}_{13} \vec{\sigma} \sigma^i \phi \vec{p}_{24} \vec{\sigma} \sigma^i + \vec{p}_{13} \vec{\sigma} \sigma^i \phi \sigma^i \vec{p}_{13} \vec{\sigma}. \quad (D13)$$

The first term in S is canceled by M from Eq. (D7), and after summing over $i = 1, 2, 3$, one obtains Eq. (55). Useful identities for Pauli matrices include

$$\sigma^i \vec{b} \vec{\sigma} \sigma^i = -\vec{b} \vec{\sigma}, \quad (D14)$$

$$\sigma^i \vec{a} \vec{\sigma} \vec{b} \vec{\sigma} \sigma^i = \vec{a} \vec{\sigma} \vec{b} \vec{\sigma} + 2\vec{b} \vec{\sigma} \vec{a} \vec{\sigma}, \quad (D15)$$

$$\sigma^i \vec{a} \vec{\sigma} \vec{b} \vec{\sigma} \vec{c} \vec{\sigma} \sigma^i = -\vec{a} \vec{\sigma} \vec{b} \vec{\sigma} \vec{c} \vec{\sigma} + 2\vec{b} \vec{\sigma} \vec{c} \vec{\sigma} \vec{a} \vec{\sigma}$$

$$- 2\vec{a} \vec{\sigma} \vec{c} \vec{\sigma} \vec{b} \vec{\sigma}. \quad (D16)$$

APPENDIX E: ANGULAR INTEGRALS

The generic form of the integrals over angles in Eq. (50) is

$$I^{ij...l} = \int d\Omega_q \frac{q^i q^j ... q^l}{(\vec{p} - \vec{q})^2}. \quad (E1)$$

Using

$$J_n = \int_{-1}^1 dz \frac{z^n}{p^2 + q^2 - 2pqz}, \quad (E2)$$

$$\gamma = \frac{p^2 + q^2}{2pq}, \quad (E3)$$

one has

$$J_n = \gamma J_{n-1} + \frac{(-1)^n - 1}{2pq n}, \quad (E4)$$

and

$$I = 2\pi J_0, \quad (E5)$$

$$I^i = 2\pi q J_1 e^i, \quad (E6)$$

$$I^{ij} = \pi q^2 [(J_0 - J_2) s_p^{ij} + 2J_2 e_p^i e_p^j], \quad (E7)$$

$$I^{ijk} = \pi q^3 (J_1 - J_3) (e_p^i s_p^{jk} + e_p^j s_p^{ik} + e_p^k s_p^{ij})$$

$$+ \pi q^3 2J_3 e_p^i e_p^j e_p^k, \quad (E8)$$

where

$$J_0 = \frac{1}{pq} \ln \frac{p+q}{|p-q|}, \quad (E9)$$

$$J_1 = \gamma J_0 - \frac{1}{pq}, \quad (E10)$$

$$J_2 = \gamma^2 J_0 - \frac{1}{pq} \gamma, \quad (E11)$$

$$J_3 = \gamma^3 J_0 - \frac{1}{pq} \left(\gamma^2 + \frac{1}{3} \right), \quad (E12)$$

and

$$e_p^i = p^i/p, \quad (E13)$$

$$s_p^{ij} = \delta^{ij} - e_p^i e_p^j. \quad (E14)$$

APPENDIX F: BASIS FUNCTIONS

The kinetic energy and harmonic oscillator interaction term are of the same form in the eigenvalue equations for all mesons,

$$2H_{osc} = \vec{p}^2 - k_p \Delta_p, \quad (F1)$$

with the spring tension k_p given in Eq. (53). The Hamiltonian that provides the basis for solving the eigenvalue equations is

$$2H_b = p^2 - k_b \Delta_p, \quad (F2)$$

The eigenfunctions of $2H_b$,

$$\phi_{nlm}(\vec{p}) = \phi_{nl}(p) Y_{lm}(\Omega_p), \quad (F3)$$

TABLE VI: Coefficients s_n and d_n in Eq. (G1) in the case of the ground state of Υ in two cases corresponding to the columns third and fourth in Table II.

n	fit to middle s_n	fit to middle d_n	fit to all s_n	fit to all d_n
1	0.913585	0.00497417	0.681293	-0.00047418
2	0.336779	0.00462106	-0.463805	-0.00282348
3	0.175768	0.00402891	-0.375752	-0.00386903
4	0.106752	0.00343707	-0.277214	-0.00426835
5	0.070100	0.00288660	-0.206969	-0.00430196
6	0.048069	0.00238820	-0.156942	-0.00411092
7	0.033778	0.00194591	-0.120185	-0.00378139
8	0.024050	0.00156114	-0.092442	-0.00337367
9	0.017232	0.00123320	-0.071130	-0.00293266
10	0.012370	0.00095950	-0.054600	-0.00249178
11	0.008872	0.00073580	-0.041742	-0.00207471
12	0.006348	0.00055667	-0.031750	-0.00169663
13	0.004528	0.00041599	-0.024019	-0.00136561
14	0.003218	0.00030752	-0.018073	-0.00108405
15	0.002280	0.00022525	-0.013529	-0.00085036
16	0.001611	0.00016375	-0.010081	-0.00066033
17	0.001136	0.00011836	-0.007481	-0.00050842
18	0.000800	0.00008518	-0.005531	-0.00038867
19	0.000563	0.00006113	-0.004076	-0.00029536
20	0.000396	0.00004378	-0.002995	-0.00022329
21	0.000278	0.00003132	-0.002196	-0.00016804
22	0.000196	0.00002239	-0.001605	-0.00012594
23	0.000138	0.00001599	-0.001171	-0.00009401
24	0.000097	0.00001140	-0.000851	-0.00006989

$$Y_{lm}(\Omega_p) = \sqrt{\frac{2l+1}{4\pi} \frac{(l-m)!}{(l+m)!}} P_l^m(\cos \theta) e^{im\phi}, \quad (F4)$$

contain the radial wave functions $\phi_{nl}(p)$ that satisfy

$$\left[p^2 - \frac{k_b}{p^2} \partial_p p^2 \partial_p + \frac{l(l+1)k_b}{p^2} - x_b \right] \phi_{nl}(p) = 0. \quad (F5)$$

In terms of the scaled variable $q = p/k_b^{1/4}$ and the eigenvalue $x_b = y\sqrt{k_b}$, the substitution $\phi(p) = \chi(q)/q$ produces

$$-\chi'' + \frac{l(l+1)}{q^2} \chi(q) + q^2 \chi = y \chi(q). \quad (F6)$$

Eigensolutions normalized to $\int dq q^2 |\psi(q)|^2 = 1$ are (L denotes generalized Laguerre polynomials and $P(n, k)$ Pochhammer symbols)

$$y = 4n + 2l + 3, \quad (F7)$$

$$\begin{aligned} \chi_{nl}(q) &= (-1)^n \sqrt{\frac{2}{\Gamma(n+l+3/2)}} \\ &\times e^{-q^2/2} q^{l+1} L_n^{l+1/2}(q^2), \end{aligned} \quad (F8)$$

$$L_n^\lambda(x) = \frac{\Gamma(\lambda+n+1)}{\Gamma(n+1)} \sum_{k=0}^n \frac{P(-n, k) x^k}{\Gamma(\lambda+k+1) k!}, \quad (F9)$$

$$P(-n, k) = \Pi_{m=0}^{k-1} (-n+m). \quad (F10)$$

TABLE VII: Coefficients s_n and d_n in Eq. (G1) in the case of J/ψ in two cases corresponding to the columns third and fourth in Table IV.

n	fit to middle s_n	fit to middle d_n	fit to all s_n	fit to all d_n
1	0.947930	0.01592964	0.918576	0.01878843
2	0.275475	0.01302155	0.332419	0.01630569
3	0.130071	0.00993031	0.170690	0.01284988
4	0.072123	0.00723324	0.099102	0.00956992
5	0.042408	0.00504458	0.060136	0.00679526
6	0.025404	0.00337759	0.036945	0.00462937
7	0.015242	0.00218240	0.022680	0.00304887
8	0.009103	0.00137141	0.013855	0.00195867
9	0.005409	0.00084597	0.008425	0.00123875
10	0.003205	0.00051695	0.005111	0.00077716
11	0.001899	0.00031504	0.003098	0.00048585
12	0.001127	0.00019206	0.001878	0.00030306
13	0.000670	0.00011710	0.001139	0.00018851
14	0.000399	0.00007128	0.000689	0.00011681
15	0.000237	0.00004325	0.000417	0.00007208
16	0.000141	0.00002616	0.000251	0.00004432
17	0.000084	0.00001577	0.000152	0.00002717
18	0.000050	0.00000949	0.000091	0.00001661
19	0.000029	0.00000570	0.000055	0.00001013
20	0.000017	0.00000342	0.000033	0.00000616
21	0.000010	0.00000205	0.000020	0.00000374
22	0.000006	0.00000122	0.000012	0.00000227
23	0.000004	0.00000073	0.000007	0.00000137
24	0.000002	0.00000044	0.000004	0.00000083

The oscillator eigenvalues and corresponding radial basis functions in momentum space, normalized to 1, are

$$x_b = (4n + 2l + 3) \sqrt{k_b}, \quad (\text{F11})$$

$$\phi_{nl}(p) = \chi_{nl}(p/k_b^{1/4}) \frac{1}{k_b^{1/8} p}. \quad (\text{F12})$$

APPENDIX G: DETAILS OF THE WAVE FUNCTIONS

This appendix provides numerical data concerning the wave functions $S(k)/k$ and $D(k)/k$ that are shown in

Figs. 5 and 6. Tables VI and VII contain coefficients s_n and d_n in the expansion of functions $S(k)$ and $D(k)$ in the basis introduced in Appendix F, with $k_b = k_p$. k_B is the Bohr momentum.

$$\begin{bmatrix} S(k) \\ D(k) \end{bmatrix} = \sum_{n=1}^{\infty} \begin{bmatrix} s_n \chi_{0\,n-1}(k/k_B) \\ d_n \chi_{2\,n-1}(k/k_B) \end{bmatrix}. \quad (\text{G1})$$

The wave functions are normalized to $\int dk (S^2 + D^2) = 1$.

[1] P. A. M. Dirac, Rev. Mod. Phys. **21**, 392 (1949).
[2] P. A. M. Dirac, in *Mathematical Foundations of Quantum Theory*, Ed. A. R. Marlow, Academic Press, New York 1978.
[3] K. G. Wilson, Nucl. Phys. Proc. Suppl. **140**, 3 (2005).
[4] S. D. Głązak, Phys. Rev. D**69**, 065002 (2004).
[5] T. Appelquist and H. D. Politzer, Phys. Rev. Lett. **34**, 43 (1975).
[6] A. De Rújula and S. L. Glashow, Phys. Rev. Lett. **34**, 46 (1975).
[7] T. Appelquist, A. De Rújula, H. D. Politzer, S. L. Glashow, Phys. Rev. Lett. **34**, 365 (1975).
[8] E. Eichten, K. Gottfried, T. Kinoshita, J. Kogut, K. D. Lane, T.-M. Yan, Phys. Rev. Lett. **34**, 369 (1975).
[9] D. Gromes, I. O. Stamatescu, Nucl. Phys. B**112**, 213 (1976).
[10] W. Fischler, Nucl. Phys. B**129**, 157 (1977).
[11] J. L. Richardson, Phys. Lett. B**82**, 272 (1979).
[12] D. P. Stanley, D. Robson, Phys. Rev. D**21**, 3180 (1980).
[13] E. Eichten, K. Gottfried, T. Kinoshita, K. D. Lane, T.-M. Yan, Phys. Rev. D**17**, 3090 (1978); Erratum-ibid. D**21**, 313 (1980).
[14] E. Eichten, K. Gottfried, T. Kinoshita, K. D. Lane, T.-M. Yan, Phys. Rev. D**21**, 203 (1980).
[15] D. Besson, T. Skwarnicki, Ann. Rev. Nucl. Part. Sci. **43**, 333 (1993).
[16] E. Eichten, C. Quigg, Phys. Rev. D**49**, 5845 (1994).
[17] M. Peter, Phys. Rev. Lett. **78**, 602 (1997).
[18] K. Zalewski, Acta Phys. Polon. B**29**, 2535 (1998).
[19] W. E. Caswell and G. P. Lepage, Phys. Lett. B**167**, 437 (1986).
[20] G. T. Bodwin, E. Braaten, and G. P. Lepage, Phys. Rev. D**51**, 1125 (1995); **55**, 5853(E) (1997).
[21] N. Brambilla, A. Pineda, J. Soto, A. Vairo, Nucl. Phys. B**566**, 275 (2000).
[22] K. Pachucki, Phys. Rev. A**56**, 297 (1997).
[23] K. Pachucki, J. Phys. B**31**, 5123 (1998).
[24] K. G. Wilson, Phys. Rev. D**10**, 2445 (1974).
[25] B. A. Thacker, G. P. Lepage, Phys. Rev. D**43**, 196-208 (1991).
[26] C. T. H. Davies et al., Phys. Rev. Lett. **92**, 022001 (2004).
[27] N. Brambilla et al., hep-ph/0412158.
[28] K. G. Wilson et al., Phys. Rev. D**49**, 6720 (1994).
[29] S. Eidelman et al., Phys. Lett. B**592**, 1 (2004); and 2005 partial update for edition 2006, available at pdg.lbl.gov.
[30] R. P. Feynman, *Photon-Hadron Interactions* (Benjamin, New York, 1972).
[31] G. P. Lepage, S. J. Brodsky, Phys. Rev. D**22**, 2157 (1980).
[32] J. Kogut, L. Susskind, Phys. Rep. C**8**, 75 (1973).
[33] S. J. Brodsky, H. C. Pauli, S. S. Pinsky, Phys. Rept. **301**, 299 (1998).
[34] S. D. Głązak, Acta Phys. Polon. B**29**, 1979 (1998).
[35] S. D. Głązak, Phys. Rev. D**63**, 116006 (2001).
[36] G. 't Hooft, Nucl. Phys. B**75**, 461 (1974).
[37] C. B. Thorn, Nucl. Phys. B**699**, 427 (2004); hep-th/0405018.
[38] C. B. Thorn, hep-th/0507213.
[39] S. D. Głązak, in *Theory of Hadrons and Light-Front QCD*, World Scientific, Singapore, 1995; p. 208.
[40] S. D. Głązak, T. Masłowski, Phys. Rev. D**65**, 065011 (2002).
[41] K. G. Wilson, Phys. Rev. D **2**, 1438 (1970).
[42] S. D. Głązak, M. Więckowski, Phys. Rev. D**66**, 016001 (2002).
[43] R. J. Perry, A. Harindranath, and K. G. Wilson, Phys. Rev. Lett. **65**, 2959 (1990).
[44] H. J. Melosh, Phys. Rev. D**9**, 1095 (1974).
[45] M. M. Brisudova, R. J. Perry, Phys. Rev. D**54**, 6453 (1996).
[46] S. D. Głązak and K. G. Wilson, Phys. Rev. D**57**, 3558 (1998).
[47] S. D. Głązak, J. Młynik, Phys. Rev. D**67**, 045001 (2003).
[48] S. D. Głązak, J. Młynik, Acta Phys. Polon. B**35**, 723 (2004).
[49] R. J. Perry and K. G. Wilson, Nucl. Phys. B**403**, 587 (1993).
[50] R. J. Perry, Ann. Phys. **232**, 116 (1994).
[51] R. J. Perry, in *Proc. of Hadrons 94*, eds. V. Herscovitz and C. Vasconcellos (World Scientific, 1995); hep-th/9407056.
[52] M. Brisudová and R. Perry, Phys. Rev. D**54**, 1831 (1996).
[53] M. M. Brisudová, R. J. Perry and K. G. Wilson, Phys. Rev. Lett. **78**, 1227 (1997).
[54] E. Braaten and H. W. Hammer, Phys. Rev. Lett. **91**, 102002 (2003).
[55] S. D. Głązak and K. G. Wilson, Phys. Rev. B**69**, 094304 (2004).
[56] J. Młynik, Ph. D. thesis, Warsaw University (2005).
[57] M. Więckowski, Ph. D. thesis, Warsaw University (2005).

[58] J. D. Bjorken, *Elements Of Quantum Chromodynamics*, Presented at the SLAC Summer Institute on Particle Physics, Stanford, Calif., Jul 9-20, 1979. Published in SLAC Summer Inst.1979:219; SLAC-PUB-2372, Dec 1979. 139pp.

[59] D. J. Gross, F. Wilczek, Phys. Rev. Lett. **30**, 1343 (1973).

[60] H. D. Politzer, Phys. Rev. Lett. **30**, 1346 (1973).

[61] S. Godfrey, J. L. Rosner, Phys. Rev. D**64**, 097501 (2001); Erratum-ibid. D**66**, 059902 (2002).

[62] S. Godfrey, J. L. Rosner, in *Gargnano 2002*, *Quark confinement and the hadron spectrum* 425-427, hep-ph/0210399.

[63] S. D. Głązek, J. Narebski, Acta Phys. Polon. B**37**, 389 (2006).

[64] M. Masłowski, Ph. D. thesis, Warsaw University (2005).

[65] J. D. Bjorken and S. D. Drell, *Relativistic Quantum Mechanics*, McGraw-Hill Book Company, New York, 1964; J. D. Bjorken and S. D. Drell, *Relativistic Quantum Fields*, McGraw-Hill Book Company, New York, 1964.